Noncore Components of the Fission Yeast -Tubulin Complex

Molecular Biology of the Cell
Vol. 17, 5075–5093, December 2006

Noncore Components of the Fission Yeast γ-Tubulin Complex[D] [V]

Andreas Anders, Paula C.C. Lourenço, and Kenneth E. Sawin

Wellcome Trust Centre for Cell Biology, Edinburgh University, Edinburgh EH9 3JR, United Kingdom

Submitted November 3, 2005; Revised September 8, 2006; Accepted September 25, 2006
Monitoring Editor: Trisha Davis

Relatively little is known about the in vivo function of individual components of the eukaryotic γ-tubulin complex (γ-TuC). We identified three genes, *gfh1+*, *mod21+*, and *mod22+*, in a screen for fission yeast mutants affecting microtubule organization. *gfh1+* is a previously characterized γ-TuC protein weakly similar to human γ-TuC subunit GCP4, whereas *mod21+* is novel and shows weak similarity to human γ-TuC subunit GCP5. We show that mod21p is a bona fide γ-TuC protein and that, like *gfh1Δ* mutants, *mod21Δ* mutants are viable. We find that *gfh1Δ* and *mod21Δ* mutants have qualitatively normal microtubule nucleation from all types of microtubule-organizing centers (MTOCs) in vivo but quantitatively reduced nucleation from interphase MTOCs, and this is exacerbated by mutations in *mod22+*. Simultaneous deletion of gfh1p, mod21p, and alp16p, a third nonessential γ-TuC protein, does not lead to additive defects, suggesting that all three proteins contribute to a single function. Coimmunoprecipitation experiments suggest that gfh1p and alp16p are codependent for association with a small "core" γ-TuC, whereas mod21p is more peripherally associated, and that gfh1p and mod21p may form a subcomplex independently of the small γ-TuC. Interestingly, sucrose gradient analysis suggests that the major form of the γ-TuC in fission yeast may be a small complex. We propose that gfh1p, mod21p, and alp16 act as facultative "noncore" components of the fission yeast γ-TuC and enhance its microtubule-nucleating ability.

INTRODUCTION

In eukaryotic cells, microtubule nucleation from both centrosomal and noncentrosomal sites is thought to be driven primarily by protein complexes containing γ-tubulin and associated proteins that are alternatively known as gamma-complex proteins (GCPs) or gamma-ring proteins (Grips) (Zheng *et al*., 1995; Murphy *et al*., 1998; Wilde and Zheng, 1999; Gunawardane *et al*., 2000; Murphy *et al*., 2001). For simplicity, in this work, we use the GCP nomenclature. In higher eukaryotes, two different γ-tubulin complexes (γ-TuCs) have been identified, and these may vary in their relative abundance in different types of cells. The smaller complex is known as the γ-tubulin small complex (γ-TuSC) and contains two copies of γ-tubulin and one copy each of GCP2 and GCP3 (Oegema *et al*., 1999; Gunawardane *et al*., 2000) The larger complex, the γ-tubulin ring complex (γ-TuRC), contains multiple copies of γ-tubulin, GCP2, and GCP3, plus the additional proteins GCP4, GCP5, and GCP6 (Fava *et al*., 1999; Oegema *et al*., 1999; Murphy *et al*., 2001). In vitro, the γ-TuRC is much more active for microtubule nucleation than the γ-TuSC (Oegema *et al*., 1999). Accordingly, the γ-TuRC has been observed to form a "lock-washer" structure that may be made up of several linked γ-TuSCs, allowing the γ-TuRC to act as a direct template for microtubule nucleation (Zheng *et al*., 1995; Gunawardane *et al*., 2000; Oakley, 2000; Schiebel, 2000; Job *et al*., 2003). However, to date there has been relatively little analysis of the relative contributions of the γ-TuRC and γ-TuSC to microtubule nucleation inside living cells; thus, it remains an open question to what extent both large and small γ-TuCs are directly involved in nucleation in vivo, and whether different complexes may be involved in different types of microtubule nucleation.

In the budding yeast *Saccharomyces cerevisiae*, γ-tubulin (Tub4p) and the GCP2 and GCP3 homologues Spc97p and Spc98p, respectively, are all essential proteins. They form a "Tub4 complex" that is recruited to the nucleoplasmic face of the spindle pole body (SPB; the yeast centrosome equivalent) by the protein Spc110p and to the cytoplasmic face of the SPB by Spc72p (Knop and Schiebel, 1998, and references therein). However, budding yeast homologues of GCP4, GCP5, and GCP6 have not been identified; thus, it is not clear whether budding yeast can serve as a useful model for understanding the function of the proteins that contribute to the formation of the larger γ-TuRC.

Unlike budding yeast, microtubule nucleation sites in the fission yeast *Schizosaccharomyces pombe* are not restricted to the SPB, but rather they are also found on the nuclear envelope and on microtubules themselves during interphase (so-called interphase microtubule-organizing centers, or iMTOCs), and at the cell division site during mitosis (the so-called equatorial microtubule-organizing center, or eMTOC; Hagan, 1998; Drummond and Cross, 2000; Tran *et al*., 2001; Sawin *et al*., 2004; Zimmerman *et al*., 2004; Janson *et al*., 2005; Sawin and Tran, 2006). The fission yeast homologues of γ-tubulin, GCP2, and GCP3 are known as gtb1p/tug1p, alp4p, and alp6p, respectively, and all three proteins are essential for viability (Horio *et al*., 1991; Stearns *et al*., 1991; Vardy and Toda, 2000). In addition, homologues of both GCP4 and GCP6 have recently been identified and characterized; these are known as gfh1p and alp16p, respectively (Fujita *et al*., 2002; Venkatram *et al*., 2004). Interestingly, although defects in microtubule distribution are apparent in both *gfh1Δ* and *alp16Δ* mutants, neither gfh1p nor

This article was published online ahead of print in *MBC in Press* (http://www.molbiolcell.org/cgi/doi/10.1091/mbc.E05–11–1009) on October 4, 2006.

[D] [V] The online version of this article contains supplemental material at *MBC Online* (http://www.molbiolcell.org).

Address correspondence to: Kenneth E. Sawin (ken.sawin@ed.ac.uk).

alp16p is essential for viability. This suggests that in fission yeast, microtubule nucleation may not absolutely require an intact large γ-TuC (we reserve the term "ring" complex for those complexes where a ring complex has been observed directly in the electron microscope). More generally, the presence of such proteins in fission yeast suggests that this organism may provide a useful system for understanding the function of these components of the γ-TuC.

Here, we describe the isolation of a novel gene, *mod21+*, which we show to be the fission yeast homologue of GCP5. Characterization of the *mod21Δ* phenotype, both singly and in combination with deletion mutants of *gfh1+* and *alp16+*, suggests that gfh1p, mod21p, and alp16p act together as "noncore" subunits of the γ-TuC, promoting the ability of the complex to drive microtubule nucleation. Biochemical characterization of all three proteins suggests that gfh1p and alp16p may cooperate in the assembly of a large γ-TuC in fission yeast, and this is consistent with our finding that nonadditive phenotypes are observed when *gfh1+*, *mod21+*, and *alp16+* are simultaneously deleted. Importantly, however, even in this triple-deletion strain, most aspects of γ-tubulin–dependent microtubule nucleation persist as normal. Because we find that γ-tubulin in wild-type fission yeast mostly seems to exist in the form of a small complex, we suggest that γ-TuCs containing noncore subunits and γ-TuCs lacking noncore subunits both contribute to microtubule nucleation in fission yeast.

MATERIALS AND METHODS

Yeast Methods

General yeast methods were as described previously (Moreno *et al*., 1991). A complete strain list is presented in Table 1. Curved cell-shaped mutants were isolated by visual screening of yeast colonies after transformation with an insertional mutagenesis cassette containing the *ura4+* gene, and sites of insertion were determined as described previously (Snaith and Sawin, 2003). Gene deletion and C-terminal epitope- or green fluorescent protein (GFP)-tagging was performed by polymerase chain reaction (PCR)-based gene targeting, by using the kanMX or natMX selectable marker for resistance to G418 and nourseothricin, respectively (Bahler *et al*., 1998; Goldstein and McCusker, 1999). *gfh1Δ::hphMX* and *mod21Δ::hphMX* hygromycin-resistant strains were generated by transforming *gfh1Δ::kanMX* and *mod21ΔkanMX* strains with a PCR-amplified hphMX cassette containing flanked regions of homology (to promoter and terminator regions) also found within the kanMX cassette (Hentges *et al*., 2005). Gene deletions and tagging were confirmed by yeast colony PCR and Western blotting as appropriate. The functionality of tagged versions of gfh1p, mod21p, alp16p, alp4p, and alp6p was determined by immunofluorescence analysis of interphase microtubule organization in both the *mod22+* and the more sensitive *mod22-1* background (Supplemental Tables 2 and 3), and this was complemented by a cell shape assay (see below). From these, gfh1-Myc, mod21-Myc, and mod21-GFP were judged to be fully functional, gfh1-GFP to be partially functional, and gfh1-HA likely to be defective or have altered function. Other strains bearing one or more tagged proteins were judged to have intermediate levels of function, to varying degrees, based on comparisons to untagged (positive control) and deletion (negative control) alleles (Supplemental Tables 2 and 3). It should be emphasized that the assay of function on the basis of microtubule organization is very sensitive and independent of assays for physical interaction by coimmunoprecipitation; in several cases, we observed what may be physiologically relevant protein–protein interactions with tagged proteins that might otherwise be considered "defective."

To generate a fission yeast strain expressing low levels of GFP-atb2p together with endogenous levels of (wild-type) untagged atb2p, we first modified a GFP-fusion protein expression plasmid, pSGA (Sawin and Nurse, 1996), to contain the weak, thiamine-repressible *nmt81* promoter (Basi *et al*., 1993) and the open reading frame of enhanced M2-GFP (Cormack *et al*., 1996), thus creating plasmid pKS72. The atb2p open-reading frame from pDQ105 (Ding *et al*., 1998) was then subcloned into pKS72, creating pKS421, which expresses the M2-GFP-atb2 from the *nmt81* promoter. pKS421 was linearized by MluI digestion to promote integration at the *ars1* locus and transformed into yeast, followed by isolation of stable integrants, which were found to exhibit uniform, low levels of GFP-atb2p expression by fluorescence microscopy and Western blotting when grown in the absence of thiamine (our unpublished data). A single isolate was used as the parent strain for subsequent strain constructions.

Immunofluorescence and Microscopy

For anti-tubulin immunofluorescence, cells were fixed in methanol at −70°C, processed as described above, and imaged by laser scanning confocal microscopy (Sawin and Nurse, 1998; Sawin *et al*., 2004). Figures show maximum projections of Z-stacks, including the entire cell volume. Live cell imaging was performed on a Nikon TE300 wide-field inverted microscope system as described previously (Snaith and Sawin, 2003; Sawin *et al*., 2004). For live cell three-channel imaging of GFP fused to γ-TuC components (either alp4p, gfh1p, mod21p, or alp16p) together with sad1-dsRed and 4,6-diamidino-2-phenylindole (DAPI), eight Z-sections at 0.6-μm intervals were collected at a single time point (800-ms exposure for GFP, 400-ms exposure for sad1 and DAPI, with appropriate neutral density filters to minimize photobleaching), and maximum projections were generated. For quantitation of microtubule bundle number in live cells expressing GFP-atb2, 10 Z-sections were collected at 0.6-μm intervals at a single time point (800-ms exposure, with neutral density filters). These images were deconvolved using softWoRx (Applied Precision, Issaquah, WA), and maximum projections of Z-sections were then generated. For time-lapse two-channel imaging of GFP-atb2p and sad1-dsRed, eight Z-sections at 0.6-μm intervals were collected every 20 s (400-ms exposure for GFP and 200 ms for sad1-dsRed, with neutral density filters) and deconvolved, and maximum projections of Z-sections were generated. For display of total SPB movement in these sequences, maximum projections from all time points of a given sequence were combined into a single average "time projection." For time-lapse single-channel imaging of GFP-atb2p (assays of astral microtubule release), eight Z-sections at 0.6-μm intervals were collected every 30 s (800-ms exposure per section, with neutral density filters). After deconvolution, maximum projections were generated. For live-cell imaging of alp4-GFP in various mutant strains, eight Z-sections at 0.6-μm intervals were collected at a single time point (400-ms exposure, with neutral density filters), and maximum projections of Z-sections were generated without deconvolution.

Physiological Experiments

For morphology experiments, cell shape defects were determined by growing cells on YE5S plates for 2 d, replica plating to fresh plates, and examining cell shape after 3 h at 32°C (Snaith and Sawin, 2003). For imaging of cell shape by differential interference contrast (DIC) microscopy, cells were washed off the plates with deionized water and immediately fixed in 3% formaldehyde.

For microtubule regrowth experiments, exponentially growing cells were chilled in an ice water bath for 30 min and transferred to 32°C for the specified time before collection by rapid filtration, fixation in methanol at −70°C, and processing for immunofluorescence and confocal imaging (Sawin *et al*., 2004). For quantitation, nucleation sites were counted in at least 150 cells per strain, at the 30-s time point.

Biochemical Methods

For immunoprecipitations, native cell extracts were prepared by freezing pelleted cells in liquid nitrogen and grinding to a powder while frozen. Frozen powder was resuspended in buffer H50 (50 mM Na HEPES, pH 7.5, 75 mM KCl, 1 mM EDTA, and 0.1% Triton X-100, plus a protease inhibitor cocktail). Extracts were clarified by microfuge centrifugation (13,000 rpm) for 15 min at 4°C, and the protein concentration was adjusted to 8 mg/ml. One milliliter of each extract was incubated with 10 μl of protein G Dynabeads suspension, preloaded with 2 μg of either hemagglutinin (HA)-antibody 12CA5, or an anti-GFP antibody. After incubation with rotation for 1 h at 4°C, beads were washed six times in 1 ml of buffer H50 and resuspended in Laemmli sample buffer for SDS-PAGE and Western blotting. In all immunoprecipitation experiments, immunoprecipitation lanes were 50× overloaded relative to total extract lanes.

For sucrose gradients, clarified extracts were prepared as for immunoprecipitation by using buffer H50 also containing 1 mM β-mercaptoethanol and 0.1 mM GTP. Sucrose gradients (5–40%) were generated in the same buffer. Gradients were loaded with 100 μl of clarified extract and centrifuged at 50,000 rpm for 4 h at 4°C in a TLS-55 rotor. Fractions (100 μl) were collected from the top of the gradient with a cut pipette tips and analyzed by Western blotting. For higher resolution gradients (Supplemental Figure 6), 200 μl of clarified extracts was loaded onto 13.2 ml 5–40% sucrose gradients and centrifuged at 28,000 rpm for 20 h at 4°C in a SW40 rotor. Fractions of 550 μl were taken from the top of the gradient by using a gradient-uploader and a fraction collector. Sedimentation coefficients were determined by parallel centrifugation of sucrose gradients containing protein standards.

For sucrose-gradient analysis of higher-eukaryotic γ-tubulin complexes, *Xenopus* egg extract was prepared as described previously (Sawin and Mitchison, 1991) and diluted fourfold in buffer H50 containing 1 mM β-mercaptoethanol and 0.1 mM GTP before loading onto gradients. *Drosophila* embryo extract was prepared by homogenizing 0–16 h *Drosophila* embryos in buffer H50 containing 1 mM β-mercaptoethanol and 0.1 mM GTP. Crude extract was clarified by centrifugation in a tabletop centrifuge (13,000 rpm for 15 min at 4°C) before loading onto sucrose gradients.

Table 1. Fission yeast strains used in this study

Strain	Genotype	Source
KS515	*ade6-M216 ura4-D18 leu1-32 h+*	Laboratory stock
KS516	*ade6-M210 ura4-D18 leu1-32 h−*	Laboratory stock
KS959	*h− gfh1Δ::kanMX6 ade6-M216 leu1-32 ura4-D18*	This study
KS963	*h− gfh1Δ::kanMX6 mod22-1 ade6-M216 leu1-32 ura4-D18*	This study
KS1107	*h− mod21Δ::kanMX6 ade6-M210 leu1-32 ura4-D18 isolate 4*	This study
KS1121	*h− mod21Δ::kanMX mod22-1 ade6-216 leu1-32 ura4-D18*	This study
KS1138	*h− alp4-3HA::kanMX ade6-216 his- leu1-32 ura4-D18*	T. Toda (Vardy *et al.*, 2000)
KS1139	*h− alp6-3HA::kanMX ade6-210 his- leu1-32 ura4-D18*	T. Toda (Vardy *et al.*, 2000)
KS1140	*h− alp4-GFP::kanMX ade6-210 his- leu1-32 ura4-D18*	T. Toda (Vardy *et al.*, 2000)
KS1225	*h+ ars1::nmt81::GFP-atb2::LEU2 ade6-210 leu1-32 ura4-D18*	This study
KS1236	*h− kanMX::nmt81::GFP-atb2 ade6-216 leu1-32 ura4-D18*	Laboratory stock (Sawin *et al.*, 2004)
KS1362	*h− gfh1Δ::kanMX mod21Δ::kanMX mod22-1 ade6-M216 leu1-32 ura4-D18*	This study
KS1365	*h− gfh1Δ::kanMX mod21Δ::kanMX ade6-M216 leu1-32 ura4-D18*	This study
KS1433	*h− gfh1-GFP::kanMX ade6-M210 leu1-32 ura4-D18*	This study
KS1466	*h− mod21-13Myc::kanMX ade6-M210 leu1-32 ura4-D18*	This study
KS1470	*h− mod22-1 ade6-210 leu1-32 ura4-D18*	This study
KS1492	*h− gfh1-3HA::kanMX ade-M210 leu1-32 ura4-D18*	This study
KS1525	*h+ alp4-13Myc::kanMX ade6-M216 leu1-32 ura4-D18*	This study
KA1527	*h+ alp6-13Myc::kanMX ade6-M216 leu1-32 ura4-D18*	This study
KS1563	*h− mod21-GFP::kanMX ade6-210 leu1-32 ura4-D18*	This study
KS1583	*h− gfh1-13Myc::kanMX ade6-M210 leu1-32 ura4-D18*	This study
KS1595	*h− gfh1-13Myc::kanMX alp6-3HA::kanMX ade6-210 leu1-32 ura4-D18*	This study
KS1597	*h− mod21-13Myc::kanMX alp6-3HA::kanMX ade6-210 leu1-32 ura4-D18*	This study
KS1599	*h+ gfh1-13Myc::kanMX alp4-3HA::kanMX ade6-216 leu1-32 ura4-D18*	This study
KS1603	*h+ mod21-13Myc::kanMX alp4-3HA::kanMX ade6-210 leu1-32 ura4-D18*	This study
KS1665	*h− alp16Δ::natMX ade6-M210 leu1-32 ura4-D18*	This study
KS1673	*h− alp16Δ::natMX mod21Δ::kanMX ade6-210 leu1-32 ura4-D18*	This study
KS1677	*h− alp16Δ::natMX gfh1Δ::kanMX ade6-M210 leu1-32 ura4-D18*	This study
KS1696	*h− mod21Δ::kanMX kanMX:nmt81:GFP-atb2 ade6-210 leu1-32 ura4-D18*	This study
KS1701	*h− mod21Δ::kanMX ars1:nmt81:GFP-atb2:LEU2 ade6-210 leu1-32 ura4-D18*	This study
KS1704	*h− gfh1Δ::kanMX kanMX:nmt81:GFP-atb2 ade6-216 leu1-32 ura4-D18*	This study
KS1708	*h− gfh1Δ::kanMX ars1:nmt81:GFP-atb2:LEU2 ade6-210 leu1-32 ura4-D18*	This study
KS1713	*h− alp16Δ::natMX gfh1Δ::kanMX mod21Δ::kanMX ade6-M210 leu1-32 ura4-D18*	This study
KS1720	*h− gfh1Δ::kanMX mod22-1 kanMX:nmt81:GFP-atb2 ade6-216 leu1-32 ura4-D18*	This study
KS1724	*h− mod21Δ::kanMX mod22-1 kanMX:nmt81:GFP-atb2 ade6-210 leu1-32 ura4-D18*	This study
KS1727	*h− gfh1Δ::kanMX mod22-1 ars1:nmt81:GFP-atb2:LEU2 ade6-210 leu1-32 ura4-D18*	This study
KS1733	*h− mod21Δ::kanMX mod22-1 ars1:nmt81:GFP-atb2:LEU2 ade6-210 leu1-32 ura4-D18*	This study
KS1762	*h− alp16Δ::natMX gfh1Δ::kanMX mod22-1 ade6-M210 leu1-32 ura4-D18*	This study
KS1764	*h− alp16Δ::natMX mod21Δ::kanMX mod22-1 ade6-M210 leu1-32 ura4-D18*	This study
KS1768	*h+ alp16Δ::natMX6 gfh1Δ::kanMX6 mod21Δ::kanMX6 mod22-1 ade6-210 leu1-32 ura4-D18*	This study
KS1804	*h+ alp16Δ::natMX mod22-1 ade6-M210 leu1-32 ura4-D18*	This study
KS1812	*h− alp16Δ::natMX6 gfh1Δ::kanMX6 mod21Δ::kanMX6 mod22-1 kanMX6:nmt81:GFP-atb2 ade6-210 leu1-32 ura4-D18*	This study
KS1817	*h− alp16Δ::natMX6 gfh1Δ::kanMX6 mod21Δ::kanMX6 mod22-1 ars1:nmt81:GFP-atb2:LEU2 ade6-210 leu1-32 ura4-D18*	This study
KS1900	*h+ gfh1-13Myc:kanMX6 ade6-216 leu1-32 ura4-D18*	This study
KS1908	*h+ mod21-13Myc:kanMX6 ade6-216 leu1-32 ura4-D18*	This study
KS1960	*h+ gfh1-3HA:kanMX6 ade6-210 leu1-32 ura4-D18* *h− gfh1-13Myc:kanMX6 ade6-216 leu1-32 ura4-D18*	This study
KS1961	*h− gfh1-13Myc::kanMX ade6-M210 leu1-32 ura4-D18* *h+ ade6-M216 ura4-D18 leu1-32*	This study
KS2003	*h+ mod21-13Myc::kanMX alp6-3HA::kanMX mod22-1 ade6-210 leu1-32 ura4-D18*	This study
KS2045	*h− mod21-13Myc::kanMX6 alp4-3HA::kanMX6 mod22-1 leu1-32 ura4-D18*	This study
KS2061	*h+ gfh1-3HA:kanMX6 mod21-13Myc::kanMX6 ade6-210 leu1-32 ura4-D18*	This study
KS2063	*h− gfh1Δ::hphMX6 mod21-13Myc::kanMX6 alp6-3HA::kanMX6 ade6-210 leu1-32 ura4-D18*	This study
KS2088	*h− mod21-13Myc::kanMX alp4-3HA::kanMX gfh1Δ::hphMX6 alp16Δ::natMX6 ade6-216 leu1-32 ura4-D18*	This study
KS2091	*h− mod21-13Myc::kanMX alp4-3HA::kanMX gfh1Δ::hphMX6 ade6-216 leu1-32 ura4-D18*	This study
KS2094	*h− mod21-13Myc::kanMX alp4-3HA::kanMX alp16Δ::natMX6 ade6-216 leu1-32 ura4-D18*	This study
KS2097	*h− mod21-13Myc::kanMX alp6-3HA::kanMX gfh1Δ::hphMX6 alp16Δ::natMX6 ade6-216 leu1-32 ura4-D18*	This study
KS2099	*h− mod21-13Myc::kanMX alp6-3HA::kanMX alp16Δ::natMX6 ade6-210 leu1-32 ura4-D18*	This study
KS2121	*h− mod21-13Myc::kanMX6 alp4-3HA::kanMX6 gfh1Δ::hphMX6 alp16Δ::natMX6 mod22-1 leu1-32 ura4-D18*	This study
KS2122	*h− gfh1-13Myc::kanMX6 alp4-3HA::kanMX6 mod21Δ::hphMX6 alp16Δ::natMX6 ade6-216 leu1-32 ura4-D18*	This study
KS2125	*h+ gfh1-13Myc::kanMX6 alp4-3HA::kanMX6 mod21Δ::hphMX6 ade6-216 leu1-32 ura4-D18*	This study

Continued

Table 1. *Continued*

Strain	Genotype	Source
KS2127	*h+ gfh1-13Myc::kanMX6 alp4-3HA::kanMX6 alp16Δ::natMX6 ade6-216 leu1-32 ura4-D18*	This study
KS2133	*h− mod21-13Myc::kanMX6 alp4-3HA::kanMX6 gfh1Δ::hphMX6 mod22-1 ade6-216 leu1-32 ura4-D18*	This study
KS2134	*h− mod21-13Myc::kanMX6 alp4-3HA::kanMX6 alp16Δ::natMX6 mod22-1 ade6-216 leu1-32 ura4-D18*	This study
KS2137	*h− mod21-13Myc::kanMX6 alp6-3HA::kanMX6 gfh1Δ::hphMX6 mod22-1 ade6-210 leu1-32 ura4-D18*	This study
KS2141	*h− gfh1-13Myc::kanMX alp4-3HA::kanMX mod22-1 ade6-216 leu1-32 ura4-D18*	This study
KS2143	*h+ gfh1-13Myc::kanMX alp6-3HA::kanMX mod22-1 ade6-210 leu1-32 ura4-D18*	This study
KS2144	*h+ gfh1-13Myc::kanMX alp6-3HA::kanMX mod21Δ::hphMX6 ade6-210 leu1-32 ura4-D18*	This study
KS2146	*h− gfh1-13Myc::kanMX alp6-3HA::kanMX alp16Δ::natMX6 ade6-210 leu1-32 ura4-D18*	This study
KS2149	*h+ gfh1-13Myc::kanMX alp6-3HA::kanMX mod21Δ::hphMX6 alp16Δ::natMX6 ade6-210 leu1-32 ura4-D18*	This study
KS2163	*h− mod21-13Myc::kanMX alp6-3HA::kanMX gfh1Δ::hphMX6 alp16Δ::natMX6 mod22-1 ade6-216 leu1-32 ura4-D18*	This study
KS2164	*h+ mod21-13Myc::kanMX alp6-3HA::kanMX alp16Δ::natMX6 mod22-1 ade6-210 leu1-32 ura4-D18*	This study
KS2171	*h− gfh1-13Myc::kanMX alp4-3HA::kanMX alp16Δ::natMX6 mod22-1 ade6-216 leu1-32 ura4-D18*	This study
KS2172	*h− gfh1-13Myc::kanMX alp4-3HA::kanMX mod21Δ::hphMX6 mod22-1 ade6-216 leu1-32 ura4-D18*	This study
KS2175	*h− gfh1-13Myc::kanMX alp4-3HA::kanMX mod21Δ::hphMX6 alp16Δ::natMX6 mod22-1 ade6-216 leu1-32 ura4-D18*	This study
KS2177	*h+ gfh1-13Myc::kanMX alp6-3HA::kanMX alp16Δ::natMX6 mod22-1 ade6-210 leu1-32 ura4-D18*	This study
KS2178	*h+ gfh1-13Myc::kanMX alp6-3HA::kanMX mod21Δ::hphMX6 mod22-1 ade6-210 leu1-32 ura4-D18*	This study
KS2179	*h− gfh1-13Myc::kanMX alp6-3HA::kanMX mod21Δ::hphMX6 alp16Δ::natMX6 mod22-1 ade6-210 leu1-32 ura4-D18*	This study
KS2260	*h− sad1-dsRed:LEU2 leu1 (sad1+)*	O. Niwa/T. Toda (Chikashige *et al.*, 2004)
KS2362	*h− gfh1Δ::kanMX6 mod22-1 alp4-GFP::natMX ade6-M216 leu1-32 ura4-D18*	This study
KS2363	*h+ gfh1Δ::kanMX6 alp4-GFP::natMX ade6-M216 leu1-32 ura4-D18*	This study
KS2402	*h− mod21Δ::kanMX6 mod22-1 alp4-GFP::natMX ade6-M216 leu1-32 ura4-D18*	This study
KS2405	*h− mod21Δ::kanMX6 alp4-GFP::natMX ade6-M216 leu1-32 ura4-D18*	This study
KS2423	*h− alp16Δ::natMX gfh1Δ::kanMX mod21Δ::kanMX alp4-GFP::natMX ade6-210 leu1-32 ura4-D18*	This study
KS2508	*h− mod21-13Myc::kanMX6 alp16Δ::natMX ade6-M210 leu1-32 ura4-D18*	This study
KS2509	*h− gfh1-3HA::kanMX6 mod21-13Myc::kanMX6 alp16Δ::natMX ade6-M210 leu1-32 ura4-D18*	This study
KS2510	*h+ gfh1-3HA::kanMX6 mod21-13Myc::kanMX6 alp16Δ::natMX ade6-M210 leu1-32 ura4-D18*	This study
KS2519	*h− alp16-3HA::kanMX6 ade6-M210 leu1-32 ura4-D18*	This study
KS2520	*h− alp16-13Myc::kanMX6 ade6-M210 leu1-32 ura4-D18*	This study
KS2528	*h− alp4-3HA::kanMX alp16-13Myc::kanMX6 ade6-216 leu1-32 ura4-D18*	This study
KS2530	*h+ alp16-3HA::kanMX6 gfh1-13Myc::kanMX6 mod21Δ::hphMX ade6-M210 leu1-32 ura4-D18*	This study
KS2539	*h− alp4-3HA::kanMX alp16-13Myc::kanMX6 gfh1Δ::hphMX6 ade6-M216 leu1-32 ura4-D18*	This study
KS2541	*h+ alp4-3HA::kanMX alp16-13Myc::kanMX6 mod21Δ::hphMX6 ade6-M210 leu1-32 ura4-D18*	This study
KS2547	*h+ alp16-3HA::kanMX6 mod21-13Myc::kanMX6 gfh1Δ::hphMX6 ade6- leu1-32 ura4-D18*	This study
KS2549	*h+ alp4-3HA::kanMX alp16-13Myc::kanMX6 gfh1Δ::hphMX6 mod21Δ::hphMX6 ade6-M210 leu1-32 ura4-D18*	This study
KS2553	*h+ alp16-3HA::kanMX6 gfh1-13Myc::kanMX6 ade6-M210 leu1-32 ura4-D18*	This study
KS2557	*h− alp16-3HA::kanMX6 mod21-13Myc::kanMX6 ade6-M210 leu1-32 ura4-D18*	This study
KS2571	*h− alp16-GFP::kanMX6 ade6-M210 leu1-32*	This study
KS2861	*h− ars1::nmt81::GFP-atb2::LEU2 sad1-dsRed:LEU2 (sad1+) ade6-210 leu1-32 ura4-D18*	This study
KS2873	*h− ars1:nmt81:GFP-atb2:LEU2 sad1-dsRed:LEU2 (sad1+) mod22-1 ade6-210 leu1-32 ura4-D18*	This study
KS2876	*h− alp16Δ::natMX6 gfh1Δ::hphMX6 mod21Δ::kanMX6 ars1:nmt81:GFP-atb2:LEU2 ade6-210 leu1-32 ura4-D18*	This study
KS2881	*h− ars1:nmt81:GFP-atb2:LEU2 mod22-1 ade6-210 leu1-32 ura4-D18*	This study
KS2884	*h− kanMX6:nmt81:GFP-atb2 mod22-1 ade6-210 leu1-32 ura4-D18*	This study
KS2887	*h+ alp4-GFP:kanMX sad1-dsRed:LEU2 leu1-32*	This study
KS2893	*h+ gfh1-GFP:kanMX sad1-dsRed:LEU2 leu1-32*	This study
KS2903	*h+ mod21-GFP:kanMX sad1-dsRed:LEU2 leu1-32*	This study
KS2917	*h− gfh1Δ::hphMX6 ars1:nmt81:GFP-atb2:LEU2 sad1-dsRed:LEU2 (sad1+) ade6-210 leu1-32 ura4-D18*	This study

Continued

Table 1. *Continued*

Strain	Genotype	Source
KS2918	*h− mod21Δ::kanMX6 ars1:nmt81:GFP-atb2:LEU2 sad1-dsRed:LEU2 (sad1+) ade6-210 leu1-32 ura4-D18*	This study
KS2919	*h− alp16Δ::natMX6 ars1:nmt81:GFP-atb2:LEU2 sad1-dsRed:LEU2 (sad1+) ade6-210 leu1-32 ura4-D18*	This study
KS2923	*h− alp16Δ::natMX6 gfh1Δ::hphMX6 mod21Δ::kanMX6 ars1:nmt81:GFP-atb2:LEU2 sad1-dsRed:LEU2 (sad1+) ade6-210 leu1-32 ura4-D18*	This study
KS2924	*h− gfh1Δ::hphMX6 mod22-1 ars1:nmt81:GFP-atb2:LEU2 sad1-dsRed:LEU2 (sad1+) ade6-210 leu1-32 ura4-D18*	This study
KS2925	*h− mod21Δ::kanMX6 mod22-1 ars1:nmt81:GFP-atb2:LEU2 sad1-dsRed:LEU2 (sad1+) ade6-210 leu1-32 ura4-D18*	This study
KS2930	*h− alp16Δ::natMX6 gfh1Δ::hphMX6 mod21Δ::kanMX6 mod22-1 ars1:nmt81:GFP-atb2:LEU2 sad1-dsRed:LEU2 (sad1+) ade6-210 leu1-32 ura4-D18*	This study
KS2946	*h− alp16Δ::natMX6 gfh1Δ::hphMX6 mod21Δ::kanMX6 kanMX6:nmt81:GFP-atb2 ade6-210 leu1-32 ura4-D18*	This study
KS2949	*h− alp16Δ::natMX6 ars1:nmt81:GFP-atb2:LEU2 ade6-210 leu1-32 ura4-D18*	This study
KS2952	*h− alp16Δ::natMX6 mod22-1 ars1:nmt81:GFP-atb2:LEU2 ade6-210 leu1-32 ura4-D18*	This study
KS2974	*h+ alp16-GFP:kanMX sad1-dsRed:LEU2 leu1-32*	This study
KS3002	*h− alp16Δ::natMX kanMX6:nmt81:GFP-atb2 ade6-210 leu1-32 ura4-D18*	This study
KS3006	*h− alp16Δ::natMX kanMX6:nmt81:GFP-atb2 mod22-1 ade6-210 leu1-32 ura4-D18*	This study
KS3123	*h− gfh1-3HA::kanMX6 mod22-1 ade6- leu1-32 ura4-D18*	This study
KS3126	*h− gfh1-13Myc::kanMX6 mod22-1 ade6- leu1-32 ura4-D18*	This study
KS3130	*h− gfh1-GFP::kanMX6 mod22-1 ade6- leu1-32 ura4-D18*	This study
KS3132	*h+ mod21-GFP::kanMX6 mod22-1 ade6- leu1-32 ura4-D18*	This study
KS3139	*h+ alp16-GFP::kanMX6 mod22-1 ade6- leu1-32 ura4-D18*	This study
KS3141	*h+ mod21-13Myc::kanMX6 mod22-1 ade6- leu1-32 ura4-D18*	This study
KS3145	*h− alp4-3HA::kanMX6 mod22-1 ade6- leu1-32 ura4-D18*	This study
KS3147	*h+ alp6-3HA::kanMX6 mod22-1 ade6- leu1-32 ura4-D18*	This study
KS3149	*h+ alp4-3HA::kanMX6 alp16-Myc::kanMX6 mod22-1 ade6- leu1-32 ura4-D18*	This study
KS3151	*h+ alp16-3HA::kanMX6 mod22-1 ade6- leu1-32 ura4-D18*	This study
KS3159	*h− alp16-13Myc::kanMX6 mod22-1 ade6- leu1-32 ura4-D18*	This study
KS3260	*h− alp4-GFP::kanMX6 mod22-1 ade6- leu1-32 ura4-D18*	This study

RESULTS

Mod21p Is a Novel Component of the Fission Yeast γ-TuC

Previously we identified two genes, *mto1+* and *mto2+*, in an insertional mutagenesis screen for cell-morphology mutants; *mto1+* was initially known as *mod20+/mbo1+* (Sawin *et al*., 2004; Venkatram *et al*., 2004, 2005; Janson *et al*., 2005; Samejima *et al*., 2005). Both mto1p and mto2p are involved in microtubule nucleation and organization via interactions with the γ-TuC, and mutants produce a curved cell phenotype after return-to-growth from stationary phase (Sawin *et al*., 2004; Samejima *et al*., 2005). In the same screen, we identified two additional mutants, *mod12* and *mod21*, that also had a curved cell phenotype but showed different characteristics relative to *mto1* and *mto2* mutants after backcrossing (our unpublished data; Figure 1A). Although *mto1* and *mto2* mutations segregated as single Mendelian traits in relation to the curved cell phenotype, both *mod12* and *mod21* mutants were found to produce curved cells only when combined with a mutation in an additional gene, which we have termed *mod22* (our unpublished data). *mod22-1* single mutants, which can be identified only by tetrad analysis, have no morphological mutant phenotype on their own (Figure 1A); we surmise that the *mod22-1* mutation, which is not in our standard "wild-type" laboratory strain, spontaneously arose in the strain used for mutagenesis.

Both *mod12* and *mod21* genes were identified by sequencing genomic DNA adjacent to the insertional disruption site (Snaith and Sawin, 2003). Database searches suggested that mod12p and mod21p were similar to γ-TuC proteins GCP4 and GCP5, respectively, although in both cases the sequence similarity was remarkably low (<20%, without even considering gaps; Supplemental Figures 1 and 2). Mod12p is identical to gfh1p, which has recently been identified and characterized as a homologue of GCP4 (Venkatram *et al*., 2004); therefore, we henceforth refer to *mod12+* as *gfh1+*. We constructed targeted gene deletions for both *gfh1+* and *mod21+*. As previously shown by Venkatram *et al*. (2004), *gfh1*Δ mutants were viable, and this was also true for *mod21*Δ mutants. As in our original mutant screen, *gfh1*Δ and *mod21*Δ mutants yielded curved cells only as double mutants in combination with *mod22-1* (Figure 1A). By immunofluorescence of fixed cells, relatively minor defects in interphase microtubule organization could be observed in *gfh1*Δ and *mod21*Δ single mutants during steady-state growth (Venkatram *et al*., 2004), whereas both *gfh1*Δ *mod22-1* and *mod21 mod22-1* double mutants showed more abnormal microtubule distributions, including fewer, thicker microtubule bundles, and often curving of microtubule bundles around cell tips (Figure 1B and Supplemental Table 1). We also found that the double mutant *gfh1*Δ *mod21*Δ did not show a stronger defective microtubule phenotype than either single mutant, and the triple mutant *gfh1*Δ *mod21*Δ *mod22-1* did not show a stronger phenotype than either *gfh1*Δ or *mod21*Δ in combination with *mod22-1*, indicating that gfh1p and mod21p are not redundant for microtubule function in fission yeast.

To confirm that mod21p is a bona fide component of the fission yeast γ-TuC, we examined its potential associations with known proteins of the γ-TuC as well as its intracellular localization. In coimmunoprecipitation experiments from fission yeast extracts, we found that Myc-tagged mod21p was physically associated with HA-tagged γ-TuC proteins alp4p (GCP2 homologue) and alp6p (GCP3 homologue), in

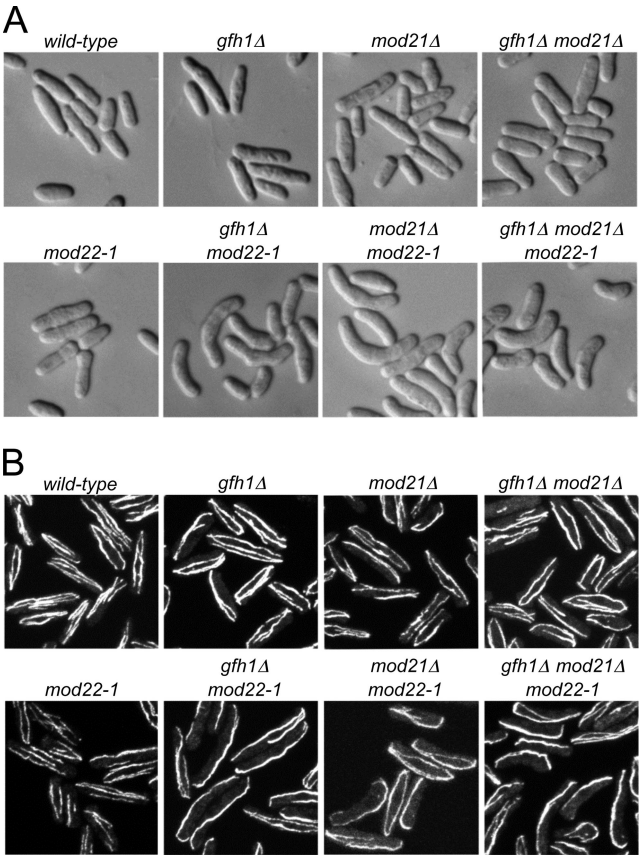

Figure 1. Cell shape and microtubule distribution in *gfh1*Δ, *mod21*Δ, and *mod22-1* single and double mutants. (A) Cell shape in strains of the indicated genotypes after growth to stationary phase on solid media, replica-plating to fresh media, and subsequent growth for 3 h. (B) Anti-tubulin immunofluorescence of asynchronous, exponentially growing cells of the indicated genotypes.

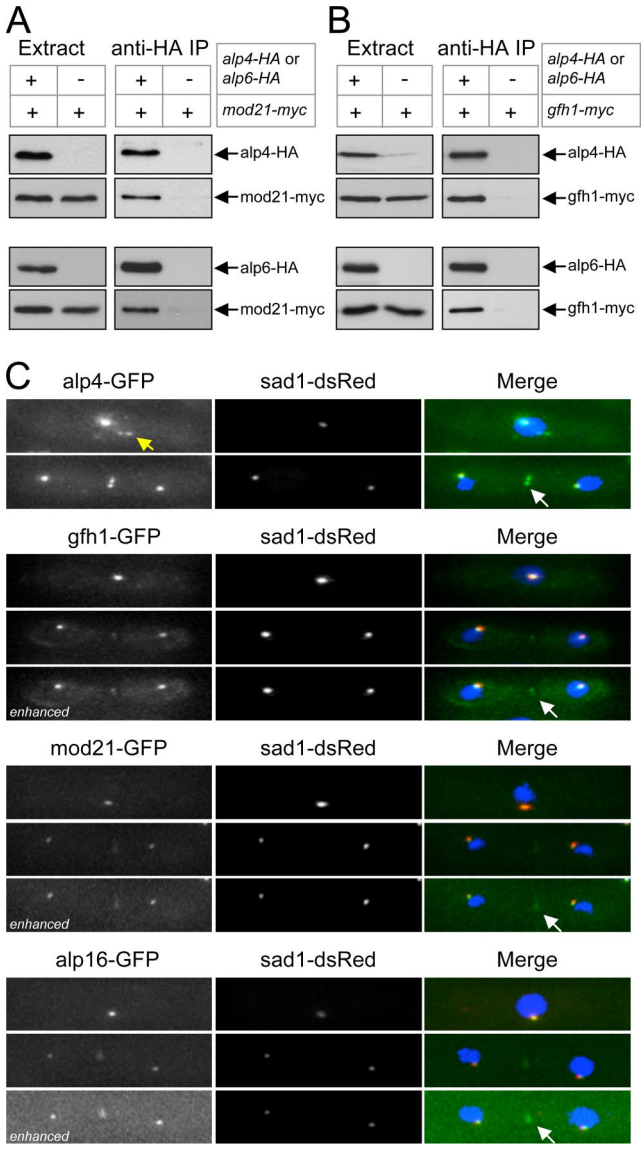

Figure 2. mod21p is a component of the fission yeast γ-TuC. (A and B) Anti-HA coimmunoprecipitation experiments from cell extracts expressing (A) Myc-tagged mod21p and (B) Myc-tagged gfh1p as well as HA-tagged alp4p or HA-tagged alp6p, as indicated. (C) Localization of GFP-tagged alp4p, gfh1p, mod21p, and alp16p (green in merge) in live cells coexpressing the SPB marker sad1-dsRed (red in merge), with DAPI counterstaining (blue in merge). In each set, interphase cells are shown above and mitotic cells below. Note interphase satellites of alp4-GFP (yellow arrow) and relatively weak eMTOC localization of gfh1p, mod21p, and alp16p relative to alp4p (white arrows). All nonenhanced images were collected and processed under identical conditions, allowing direct comparison of intensities. Enhanced images were individually altered to highlight faint eMTOC localization.

the same manner as Myc-tagged gfh1p (Figures 2, A and B, and 10; see *Materials and Methods* and Supplemental Tables 1–3 for an assessment of the functionality of these and other tagged strains).

Previous work has shown that alp4p fused to GFP is localized to SPBs throughout the cell cycle, to eMTOCs during cell division, and to iMTOC satellites along cytoplasmic microtubules during interphase (Vardy and Toda, 2000; Zimmerman *et al*., 2004; Janson *et al*., 2005; Samejima *et al*., 2005). To further confirm that mod21p is a γ-TuC protein, we examined the localization of mod21-GFP in live cells coexpressing the SPB marker sad1-dsRed (Chikashige *et al*., 2004) and compared this directly with alp4-GFP, gfh1-GFP, and alp16-GFP localization under the same imaging conditions (Figure 2C). We observed mod21-GFP at both SPBs, and, with slight image enhancement, at eMTOCs. We were unable to detect any mod21-GFP interphase satellites. Essentially the same localization was seen for gfh1-GFP and alp16-GFP (Fujita *et al*., 2002; Venkatram *et al*., 2004). Collectively, these biochemical and cytological results indicate that mod21p is part of the fission yeast γ-TuC.

In general, the fluorescence intensity of alp4-GFP at SPBs and eMTOCs was higher than that of gfh1-GFP, mod21-GFP, and alp16-GFP. This could indicate that alp4-GFP is more abundant than gfh1-GFP, mod21-GFP, and alp16-GFP at these sites. Alternatively, it is possible that GFP-tagging might negatively affect the localization of gfh1-GFP, mod21-GFP, and alp16-GFP to SPBs and eMTOCs. Indeed, additional experiments suggest that gfh1-GFP and possibly alp16-GFP (but not mod21-GFP) may have somewhat impaired function relative to untagged proteins (see *Materials and Methods* and Supplemental Tables 1–3).

Previously it has been shown that GCP4 is likely present in more than one copy in the human γ-TuC, whereas GCP5 is single-copy (Murphy *et al*., 2001). We therefore performed coimmunoprecipitations from diploid strains in which the

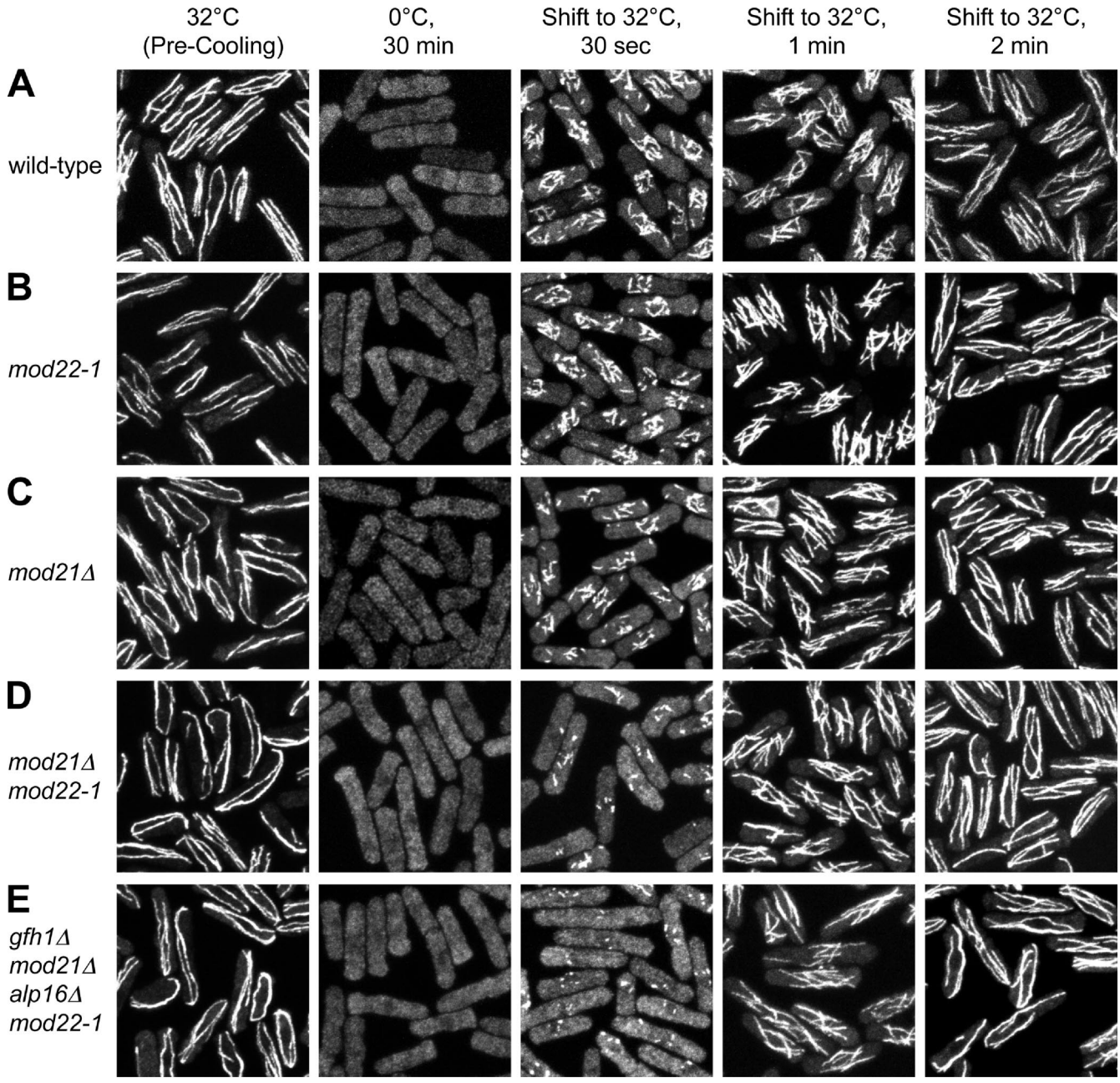

Figure 3. Microtubule renucleation in wild-type and *mod21*Δ, *mod22-1*, and multiple mutant cells. Fixed time-point images of representative strains after cold-induced microtubule depolymerization and regrowth. Note that the number of apparent nucleation sites is reduced in *mod21*Δ (C) relative to wild-type (A) and *mod22-1* (B) and further reduced in *mod21*Δ *mod22-1* (D) and *gfh1*Δ *mod21*Δ *alp16*Δ *mod22-1* (E) strains.

different alleles of gfh1p and mod21p were fused to both GFP- and Myc-tags. In these experiments, gfh1-GFP was able to coimmunoprecipitate both mod21-Myc and gfh1-Myc, whereas mod21-GFP was able to coimmunoprecipitate gfh1-Myc but not mod21-Myc (Supplemental Figure 3). Subject to the caveat that gfh1-GFP may have impaired function, this suggests that gfh1p may be multicopy in the fission yeast γ-TuC, whereas mod21p is only single copy.

gfh1p, mod21p, and alp16p All Contribute to a Single Function in Interphase Microtubule Organization and Nucleation

Neither gfh1p nor alp16p, the fission yeast homologue of the mammalian γ-TuC protein GCP6, is essential for viability, but deletion of either gene leads to defects in microtubule organization (Fujita *et al*., 2002; Venkatram *et al*., 2004). Because there has generally been relatively little in vivo characterization of the specific roles of GCP4, GCP5, or GCP6 in any eukaryote, we wanted to determine whether all or a subset of these proteins might be functionally redundant. Interestingly, we were able to construct a viable quadruple mutant *gfh1*Δ *mod21*Δ *alp16*Δ *mod22-1* strain, as well as all possible double and triple mutants, without difficulty. We also tested in more detail whether multiple mutations in any of these genes might produce a stronger microtubule-defective phenotype than single mutations. Immunofluorescence experiments in exponentially-growing cells showed that all

possible combinations of deletions of *gfh1*+, *mod21*+, and *alp16*+ were roughly similar to each other with regard to microtubule distribution; in addition, we found that when, and only when, any of these deletions or combination of deletions was combined with the *mod22-1* mutation, the microtubule phenotype became significantly worse (Figure 1B, Supplemental Figure 4, and Supplemental Table 1; also see Figure 3).

We next wanted to examine microtubule nucleation in these combinations of *gfh1*Δ, *mod21*Δ, *alp16*Δ, and *mod22-1* mutants. When wild-type cells are cooled to 0°C, microtubules depolymerize within a few minutes, and when these cells are rewarmed to normal culture temperature, microtubules are rapidly nucleated from multiple sites on the surface of the cell nucleus (Mata and Nurse, 1997; Chen *et al*., 1999; Sawin *et al*., 2004; Pardo and Nurse, 2005; Samejima *et al*., 2005). Previous work by us and others suggests that this reflects nucleation of new microtubules rather than elongation of existing microtubule "stubs." First, although a small number of stubs are typically observed near the nucleus after drug-induced depolymerization (Tran *et al*., 2001; Sawin and Snaith, 2004; Janson *et al*., 2005), these are not seen after cold-induced depolymerization; that is, even when small increases in the total soluble tubulin pool (due to depolymerization) are obvious by immunofluorescence, there are no fluorescence "hot spots" near the nucleus that would indicate subresolution microtubule stubs (Sawin *et al*., 2004; Samejima *et al*., 2005; Figure 3). Second, in previous work characterizing the microtubule nucleation proteins mto1p and mto2p, it was found that even though *mto1*Δ and *mto2*Δ mutant cells can have varying numbers of microtubule bundles before cold treatment, in *mto2*Δ mutants recovering from cold treatment, only the SPB is active for cytoplasmic microtubule nucleation, whereas in recovering *mto1*Δ mutants, all cytoplasmic nucleation is abolished, with new microtubule nucleation occurring only from the nucleoplasmic face of the SPB and microtubules eventually breaking through the nuclear envelope into the cytoplasm (Sawin *et al*., 2004; Samejima *et al*., 2005; Zimmerman and Chang, 2005). Such strong defects would not be expected if recovery were driven by elongation of preexisting stubs, especially because microtubule bundles in *mto1*Δ and *mto2*Δ mutants generally seem to be more stable than in wild-type cells (Janson *et al*., 2005; Zimmerman and Chang, 2005). Finally, it has been shown previously that new microtubule nucleation after cold treatment in wild-type cells results from recruitment of the γ-TuC to the nuclear surface, brought about by the association of the γ-TuC with the microtubule nucleation protein mto1p, which, unlike tubulin, does visibly redistribute to the nuclear surface as a result of cold treatment, before rewarming (Sawin *et al*., 2004). We therefore used microtubule regrowth after cold treatment as an initial assay for how gfh1p, mod21p and alp16p may contribute to microtubule nucleation in vivo, in both *mod22*+ and *mod22-1* backgrounds.

In all combinations of *gfh1*Δ, *mod21*Δ, *alp16*Δ, and *mod22-1* mutants, we observed microtubule nucleation from multiple sites on the nuclear surface upon recovery from cold treatment, indicating that these genes are not essential for formation of the multiple, distributed nucleation sites seen in wild-type cells (Figure 3; our unpublished data). However, mutants that showed more aberrant microtubule distributions during exponential growth (e.g., *mod21*Δ *mod22-1* double mutants, or *gfh1*Δ *mod21*Δ *alp16*Δ *mod22-1* quadruple mutants) were also more impaired in the earliest stages of microtubule regrowth (Figure 3, D and E). In these experiments, we also quantitated the number of apparent microtubule nucleation sites at the earliest time points (Figure 4).

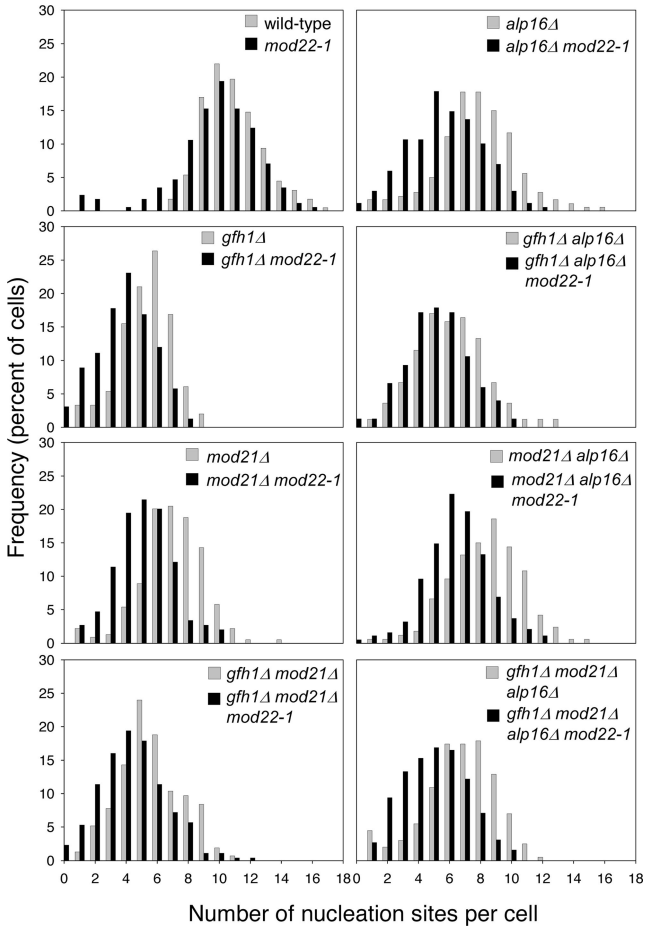

Figure 4. Quantitation of microtubule renucleation in wild-type and mutant cells. Number of microtubule nucleation sites after 30 s of microtubule regrowth in the strains shown in Figure 3 as well as in eleven additional mutant strains, as indicated. At least 150 cells were scored for each genotype.

Relative to wild-type cells, we observed reductions in the number of nucleation sites in *gfh1*Δ, *mod*21Δ and *alp1*6Δ single mutants, and similar reductions in multiple mutants. Due to inherent difficulties in scoring nucleation sites at the light-microscopic level, there was some variation in the number of apparent sites in different mutants, but we did not observe any strong synthetic effects after multiple deletion of *gfh1*+, *mod21*+, and *alp16*+. Interestingly, when single- or multiple-deletion mutants were combined with the *mod22-1* mutation, the number of nucleation sites was typically further reduced (Figure 4), whereas *mod22-1* single mutants themselves were not significantly different from wild-type cells. Together, these results suggest that gfh1p, mod21p, and alp16p are likely to contribute to a single common function in microtubule behavior and/or nucleation, and that *mod22*+ is also important for nucleation.

Microtubule Behavior In Vivo

To complement these fixed cell studies, we analyzed microtubule organization in live cells expressing GFP fused to atb2p, the minor, nonessential fission yeast α-tubulin (Ding *et al*., 1998). To reduce the likelihood of artifacts due to unforeseen effects of GFP-tubulin expression (Sawin *et al*., 2004), we used two different GFP-tubulin strains. Both strains uniformly expressed low levels of integrated GFP-

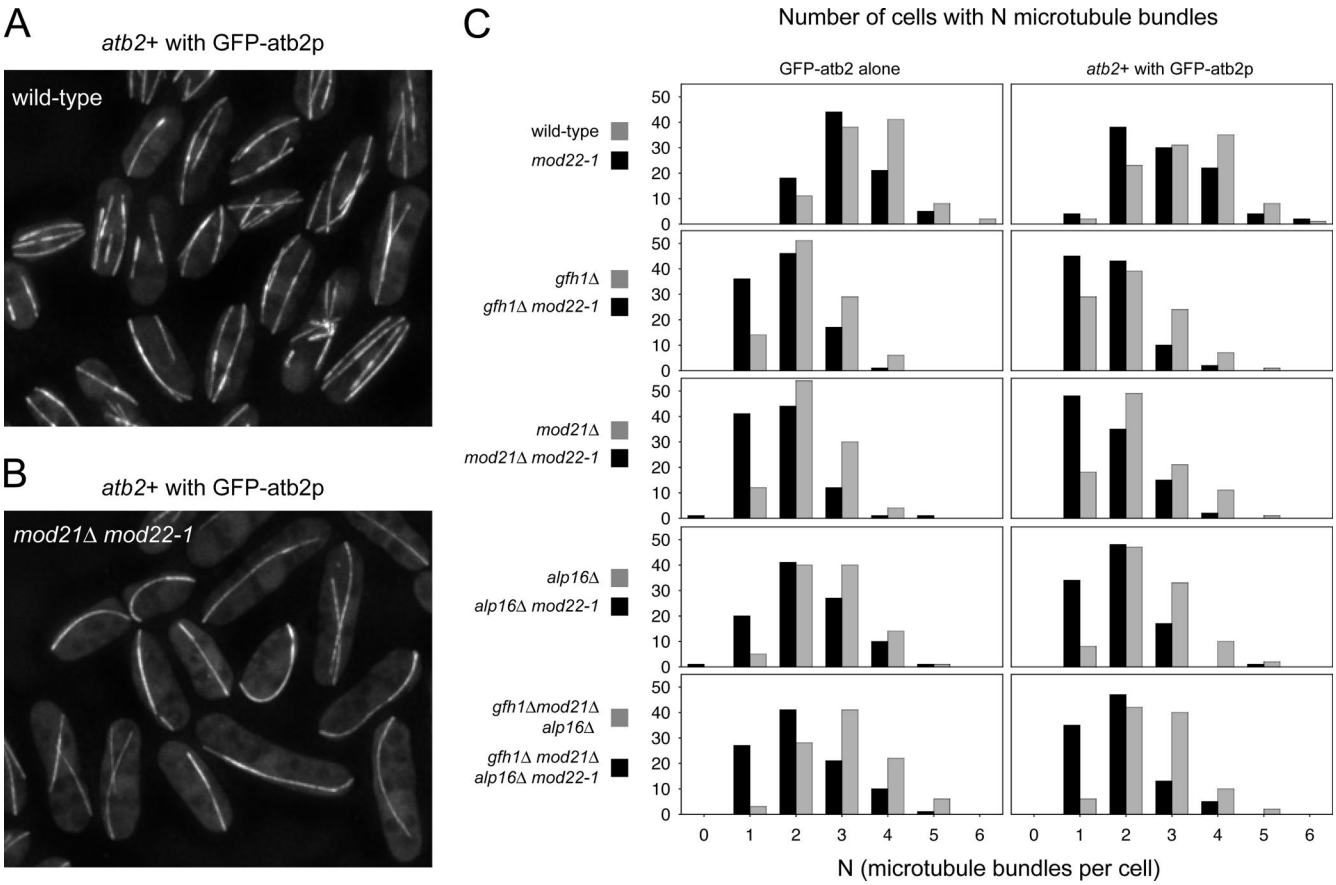

Figure 5. Reduced numbers of interphase microtubule bundles in *gfh1*Δ, *mod21*Δ, *alp16*Δ, and multiple-mutant cells. (A and B) Examples of live wild-type (A) and *mod21*Δ *mod22-1* mutants (B), expressing GFP-atb2p together with endogenous untagged atb2p. (C) Number of interphase microtubule bundles per cell in the strains indicated, expressing either GFP-tagged atb2p in conjunction with endogenous untagged atb2p, or GFP-atb2p alone. One hundred cells were scored for each strain.

atb2, in one case in place of wild-type atb2p (Sawin *et al*., 2004), and in the other case in conjunction with wild-type atb2p (see *Materials and Methods*). Essentially identical results were obtained with both GFP-tubulin strains. In cells growing at steady state, differences in microtubule organization were readily apparent comparing wild-type cells to *gfh1*Δ, *mod21*Δ and *alp16*Δ single mutants (i.e., in *mod22+* backgrounds; Figure 5, A and B; our additional unpublished data). Although most wild-type cells contained two to four microtubule bundles per cell (Drummond and Cross, 2000; Tran *et al*., 2001), *gfh1*Δ and *mod21*Δ and *alp16*Δ single mutants generally contained one to three bundles (Figure 5C). The *mod22-1* mutation by itself reduced the number of bundles only very modestly, but when it was combined with any of the *gfh1*Δ, *mod21*Δ, or *alp16*Δ single mutations, a high proportion of double-mutant cells contained only a single microtubule bundle (Figure 5C), consistent with our previous observations that *mod22-1* exacerbates the deletion-mutant phenotypes. We also analyzed the multiple mutant *gfh1*Δ *mod21*Δ *alp16*Δ in both *mod22+* and *mod22-1* backgrounds. Consistent with our previous observations of nonadditive phenotypes, the number of microtubule bundles per cell in *gfh1*Δ *mod21*Δ *alp16*Δ mutants was not further reduced relative to any of the single mutants, and as with single mutants, the *mod22-1* mutation further reduced the number of bundles in the *gfh1*Δ *mod21*Δ *alp16*Δ mutants (Figures 4 and 5C).

Interestingly, in these experiments, we did not observe cells completely lacking microtubules (i.e., cells with zero bundles), even in cases where the number of "single-microtubule bundle" cells approached 50% (Figure 5C). This deviation from Poisson statistics indicates that *gfh1*Δ, *mod21*Δ, *alp16*Δ, and *mod22-1* mutations do not simply "generally reduce" the average number of bundles per cell. Rather, these mutations reduce the likelihood that a cell will have more than one bundle. From a more mechanistic perspective, this could imply that the mutant cells contain one single site that is more likely than others to nucleate microtubules. Such a hypothetical site could in theory be responsible for all microtubule bundles in vivo, even in cells with more than one bundle, via mechanisms such as microtubule nucleation-and-release (Keating and Borisy, 1999) or microtubule bend-breakage (Sawin *et al*., 2004).

Because the most likely candidate for such a hypothetical "unique nucleation site" was the SPB, we coimaged GFP-atb2 and the SPB marker sad1-dsRed in wild-type cells; single-mutant *gfh1*Δ, *mod21*Δ, and *alp16*Δ cells; and triple-mutant *gfh1*Δ *mod21*Δ *alp16*Δ cells, both in *mod22+* and *mod22-1* backgrounds, by time-lapse microscopy. Interestingly, we found that in all mutants, new cytoplasmic microtubules could be nucleated at sites away from the SPB, as also occurs in wild-type cells (Figure 6, C, D, E, F, I, J, K, and L, white arrows; and Supplemental Movies 1–10; additional data not shown). This directly discounts the simple model

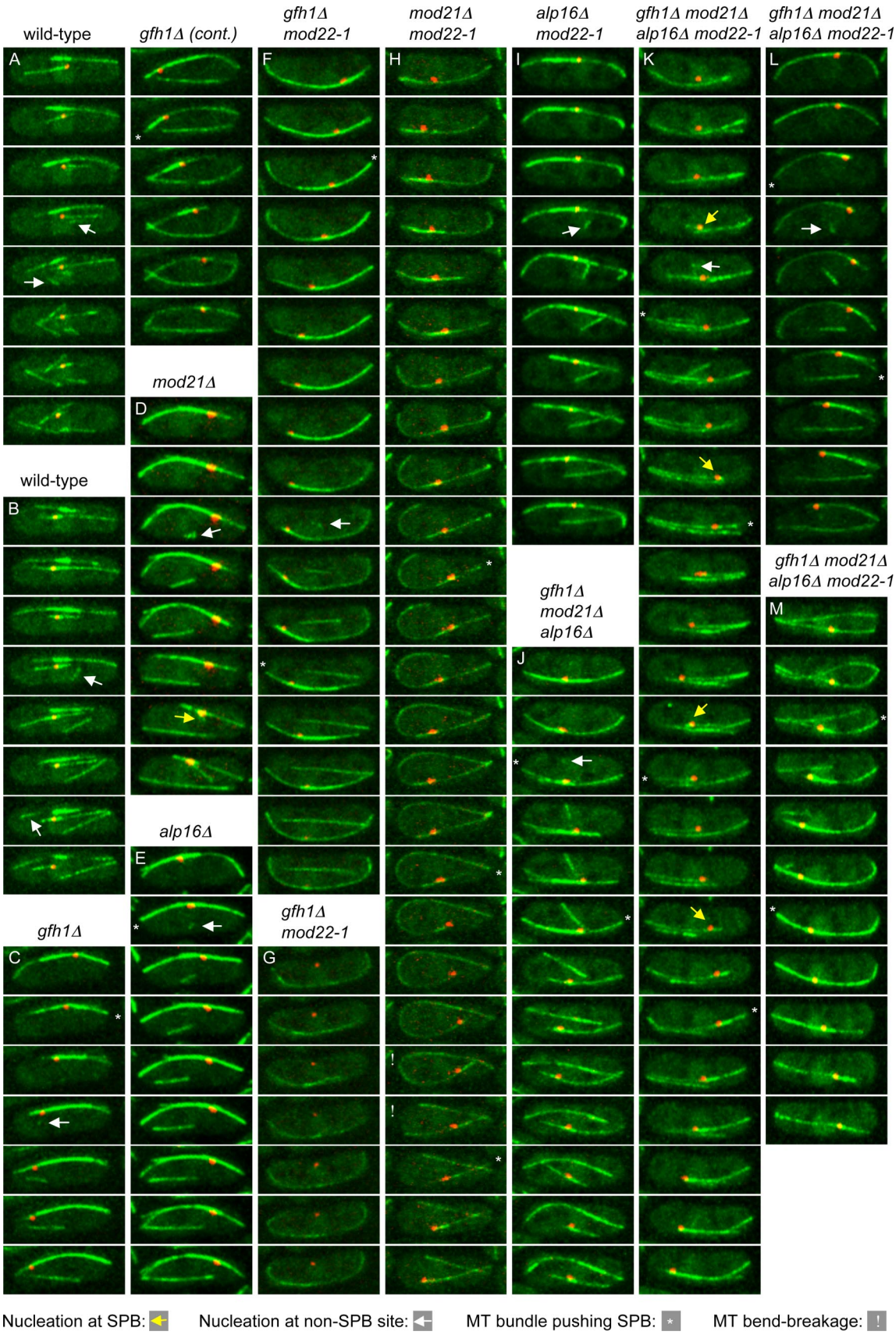

Figure 6. Microtubule nucleation and SPB behavior in wild-type and mutant cells. Stills from movies imaging GFP-atb2p (expressed together with endogenous untagged atb2p) and sad1-dsRed, at 20-s intervals, in cells of the indicated genotypes (see *Materials and Methods*). Yellow arrows indicate representative (but not all) examples of nucleation from the SPB, and white arrows indicate nucleation from non-SPB

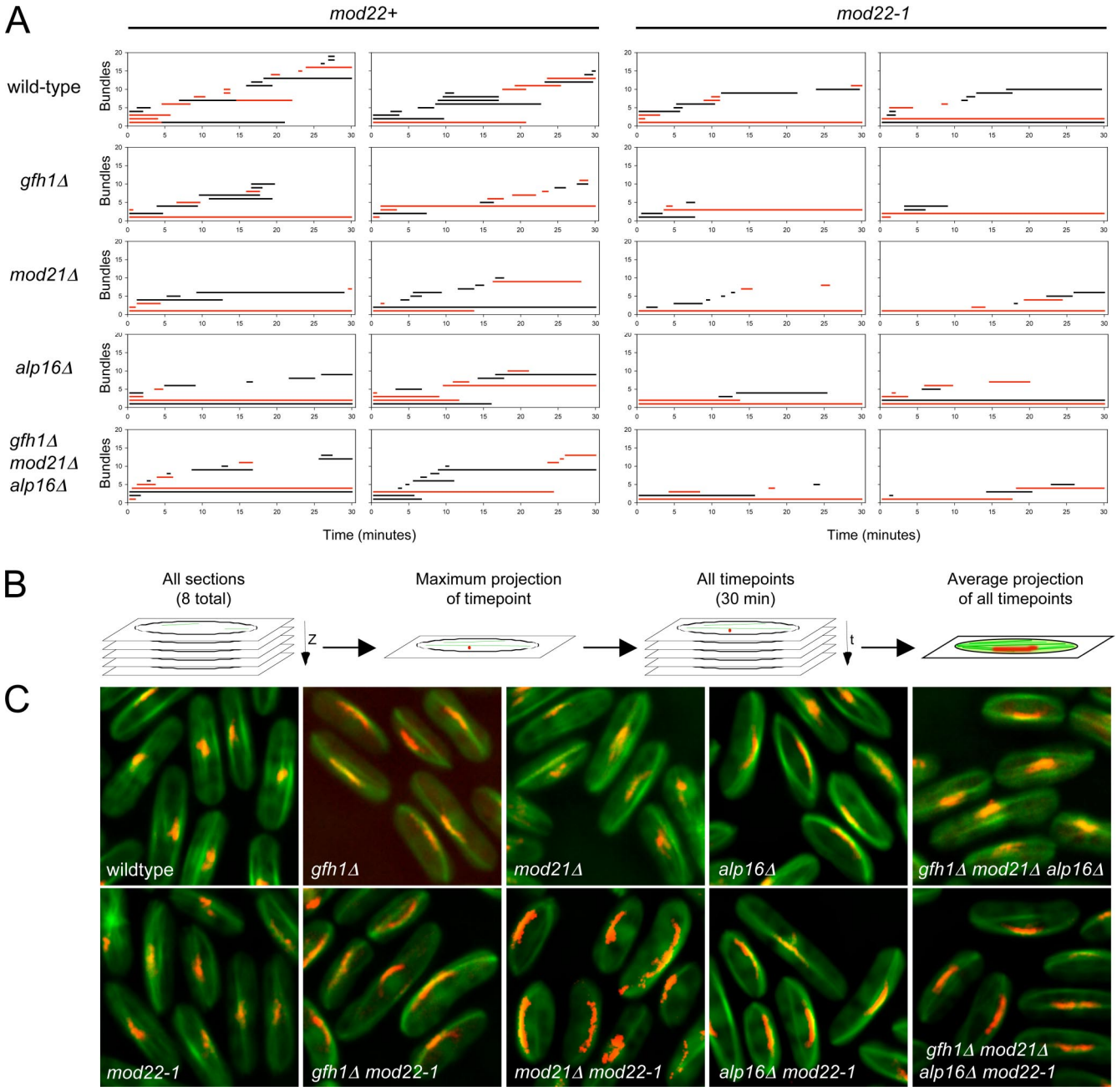

Figure 7. Microtubule bundle dynamics and SPB oscillations in wild-type and mutant cells. (A) Microtubule bundle appearance and lifetimes. Each graph shows the times of appearance and the lifetimes of microtubule bundles in a representative single cell of the indicated genotype, from a 30-min time-lapse sequence imaging both GFP-atb2 and sad1-dsRed (see *Materials and Methods*). Two cells are shown for each genotype, with *mod22+* strains on the left-hand side and *mod22-1* strains on the right-hand side. Microtubule bundles associated with the SPB are shown in red. (B) Schematic of how time-projection images were created to display SPB oscillations. (C) Average time-projection images of wild-type and mutant cells, from 30-min time-lapse sequences imaging both GFP-atb2 and sad1-dsRed. In wild-type and *mod22-1* cells, only small movements are observed.

Figure 6 (cont). sites. Asterisks indicate instances where SPB movement (away from asterisk in subsequent frames) seems to be driven by a trailing microtubule bundle pushing against the cell cortex. Note the absence of SPB movement in a rare case (G) in which the SPB is not associated with microtubules. In another case (K), the SPB is initially stationary and not associated with microtubules, but later a microtubule grows leftward and subsequently the SPB initiates rightward movement; this process is repeated several times, in both directions. Exclamation marks in H indicate a relatively rare instance of microtubule bend breakage, in this case in a *mod21Δ mod22-1* mutant.

that the SPB might be the only cytoplasmic microtubule nucleation site in the mutants.

However, time-lapse imaging also revealed several distinct properties of microtubule bundles in mutant cells as opposed to wild-type cells. Many of these differences are easily seen by plotting the appearance and duration of bundles over time in individual cells, as shown in Figure 7A. Although microtubule bundles in mutant cells were clearly dynamic, undergoing both growth and shrinkage (Figure 6,

Table 2. Frequency of microtubule nucleation events in vivo

Strain	Interphase MT nucleation events during 30-min time-lapse sequence	
	mod22+ background	*mod22-1* background
Wild type	14.5 ± 2.46	9.6 ± 1.65
*gfh1*Δ	7.4 ± 1.90	4.3 ± 1.06
*Mod21*Δ	6.5 ± 1.43	4.0 ± 1.41
*alp16*Δ	7.5 ± 1.51	4.6 ± 1.17
*gfh1*Δ *mod21*Δ *alp16*Δ	7.0 ± 2.16	4.6 ± 1.51

Numbers indicate mean ± SD for each of the 10 strains indicated. Ten cells were scored for each strain.

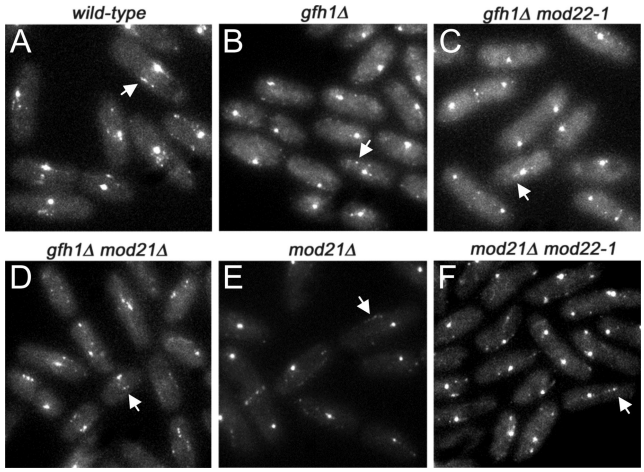

Figure 8. Alp4-GFP interphase satellites are present in *gfh1*Δ and *mod21*Δ mutants. Alp4-GFP localization in live wild-type (A) and mutant (B–F) cells of the indicated genotypes. Bright spots are SPBs; arrows indicate representative satellites. All images were collected and processed under identical conditions.

C–M; Supplemental Movies 2–5 and 7–10), some bundles were present for very long periods relative to those in wild-type cells (Figure 7A). Indeed, in most mutant cells, one or two bundles persisted throughout the entire time-lapse sequences, making it impossible to determine an "average" bundle lifetime in mutants (Figure 7C). Interestingly, these long-lived bundles were usually associated with the SPB (Figure 7A), suggesting that the SPB is likely the most prominent nucleator in these cells, although, as described above, not the only nucleator. In addition, from Figure 7A it is evident that in mutant cells, new bundles, which are as often as not associated with the SPB, occur less frequently relative to wild-type cells. Further quantitation of differences revealed that deletion of *gfh1+*, *mod21+* and/or *alp16+* reduced the frequency of new bundle appearance approximately two-fold relative to wild-type cells, and, independently of this, the *mod22-1* mutation reduced the frequency approximately 1.5-fold (Table 2). Overall, these results suggest that SPB-mediated cytoplasmic microtubule nucleation is intact in *gfh1*Δ, *mod21*Δ and *alp16*Δ mutants and that although non-SPB-mediated microtubule nucleation also occurs in the mutants, it does so less frequently than in wild-type cells.

In these experiments, we also observed strong oscillatory movements of the SPB in mutant cells compared with wild-type cells (Figures 6 and 7C and Supplemental Movies 2–5 and 7–10). Oscillations were particularly strong in cells with a single persistent SPB-associated bundle (see examples in Figure 7C), and from the varied microtubule distributions of individual cells, we could infer that oscillations are dependent on association of the SPB with microtubules (Figure 6G) and that they are probably driven by microtubule pushing (Figure 6, C, E, F, H, J, K, L, and M). Large oscillations of the SPB were first described in the context of "horsetail" movements of the nucleus during meiotic prophase (Ding *et al*., 1998), and more recently oscillations have been observed in vegetative cells under various conditions affecting microtubule organization, including ectopic expression of the meiosis-specific microtubule-organizing protein mcp6p/hrs1p, deletion of *mto2+*, and overexpression of the carboxy terminus of alp4p (Janson *et al*., 2005; Tanaka *et al*., 2005; Masuda *et al*., 2006). Our observations are consistent with these and suggest that SPB oscillations are most likely a general, indirect consequence of having a long-lived dynamic microtubule bundle associated with the SPB.

An additional indicator of non-SPB–mediated microtubule nucleation in fission yeast is the presence of iMTOC satellites on microtubules themselves (Sawin *et al*., 2004; Zimmerman *et al*., 2004; Janson *et al*., 2005; Samejima *et al*., 2005). For example, microtubule-associated satellites of GFP-tagged alp4p are visible in wild-type cells, but not in *mto2*Δ mutants, which are defective in non-SPB–mediated microtubule nucleation (Janson *et al*., 2005; Samejima *et al*., 2005), and it has recently been observed that new microtubules can be nucleated from such satellites, although this may be difficult to detect routinely (Janson *et al*., 2005). We observed alp4-GFP satellites in *gfh1*Δ and *mod21*Δ mutants, both in *mod22+* and *mod22-1* backgrounds (Figure 8), consistent with our observations of microtubule behavior in vivo.

*gfh1*Δ, *mod21*Δ, and Multiple Mutants Do Not Release Astral Microtubules

The initial characterization of gfh1p by Venkatram *et al*. (2004) suggested that it has a specific role in anchoring astral microtubules to SPBs during mitosis. Because *mod22* is an important modifier of the *gfh1*Δ phenotype, we examined potential release of astral microtubules in both *gfh1*Δ and *gfh1*Δ *mod22-1* cells expressing GFP-tubulin as well as in other mutants (Figure 9 and Table 3). However, we did not observe significant release of astral microtubules from SPBs in *gfh1*Δ mutants. Release from SPBs was occasionally observed (Figure 9B and Supplemental Movie 13), but this was equally rare in both wild-type and *gfh1*Δ cells and was not altered by either the mode of GFP-atb2p expression or *mod22* status (Table 3 and Supplemental Movies 11–15). We also examined potential release of astral microtubules in *mod21*Δ mutants, both in *mod22+* and *mod22-1* backgrounds, and in the *gfh1*Δ *mod21*Δ *alp16*Δ *mod22-1* quadruple mutant. Again, we failed to observe a significant increase in the frequency of astral microtubule release relative to wild-type cells (Table 3 and Supplemental Movies 16–19). In total, we observed either no or one astral microtubule release events in 29 eligible astral microtubule histories from wild-type cells, and between two and nine release events in 276 eligible histories from mutant cells (most events in mutant cells were questionable; see Table 3 for details). From these results, we conclude that release of astral microtubules is not an intrinsic property of *gfh1*Δ, *mod21*Δ, or *alp16*Δ mutants, either in a wild-type or *mod22-1* background. In all strains, we often observed single microtubules nucleated from the eMTOC toward the end of mitosis, during the earliest stages of

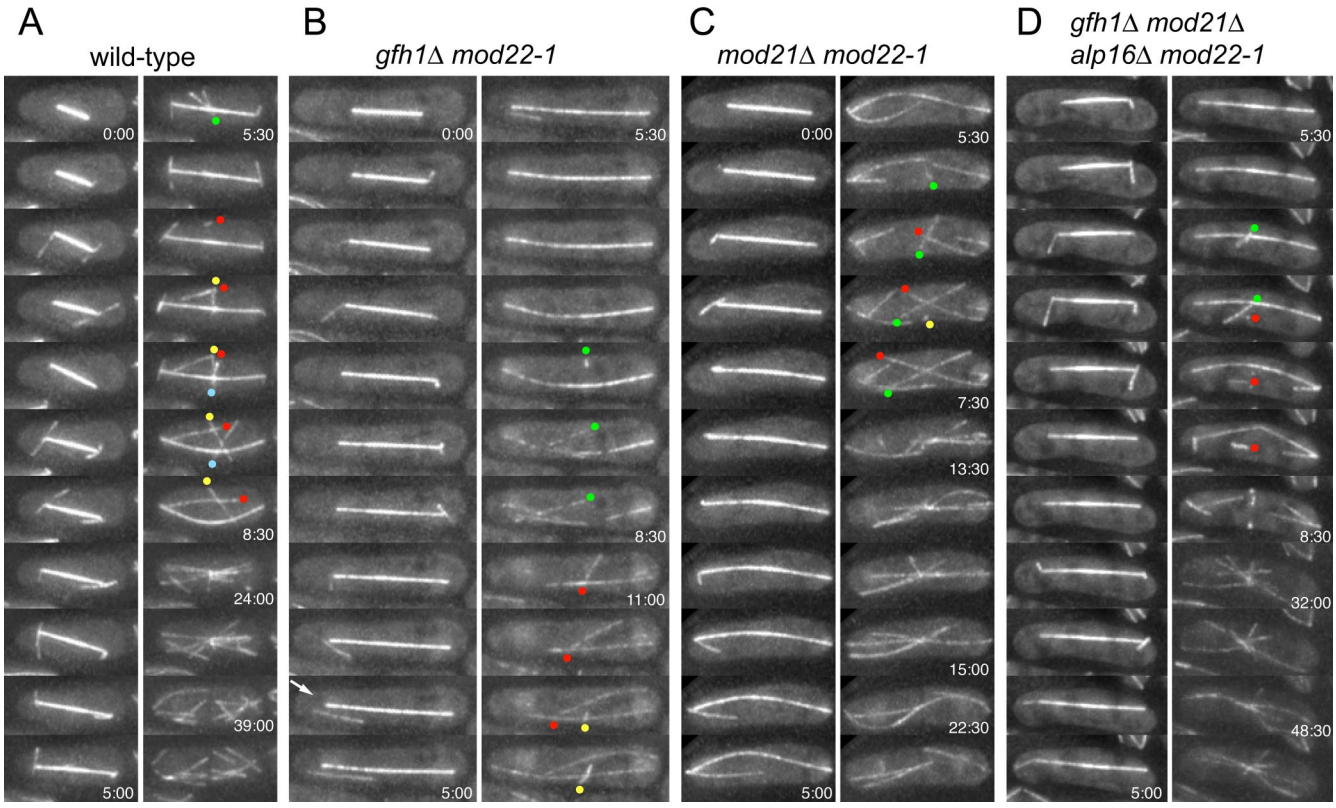

Figure 9. Microtubule behavior at the end of mitosis. Stills from movies of wild-type (A) and mutant (B–D) cells toward the end of mitosis. Time indicates minutes and seconds relative to the first time point shown; unless indicated, the time between successive frames is 30 s. Note that astral microtubules tend to be short-lived. Arrow in B indicates rare release of an astral microtubule from the spindle pole body. Note also that microtubules are sporadically "fired" from the equatorial MTOC in the center of the cell before formation of a well-formed postanaphase array. Colored dots indicate the presumed minus ends of these microtubules, with a single color for each such microtubule. In some cases, these microtubules seem to translocate away from the nucleation site, both in wild-type and mutant cells. All cells shown express both GFP-atb2p and endogenous atb2p.

formation of the postanaphase array (PAA; see below). Although these might be mistaken for released astral microtubules, with appropriate time resolution they were clearly not astral microtubules but rather early PAA microtubules (Figure 9 and Supplemental Movies 11–19).

In the course of these mitotic cell experiments, we also followed the formation of the PAA at the end of mitosis in wild-type and mutant cells. Although some variation in PAA formation was observed within all strains, no obvious consistent differences were seen in mutants relative to wild-type cells (Supplemental Movies 11–19; our additional unpublished data).

In summary, our results from both live and fixed cell experiments indicate that deletion of *gfh1+*, *mod21+* and/or *alp16+*, either individually or in combination, does not affect major qualitative aspects of microtubule nucleation and dynamics, including the appearance of interphase microtubule nucleation sites, mitotic spindle assembly, astral microtubule behavior and postanaphase array formation. Rather, deletion of these genes, especially in combination with the *mod22-1* mutation, leads to a more quantitative reduction in the number of apparent interphase microtubule nucleation sites or iMTOCs—specifically, non-SPB sites. We interpret this to indicate that gfh1p, mod21p, and alp16p may function to promote the efficiency of microtubule nucleation by the γ-TuC, thereby increasing the number of active microtubule nucleation sites in vivo.

Organizational State of the Fission Yeast γ-TuC In Vivo

One potential explanation for the nonadditive defective microtubule phenotype seen in the *gfh1Δ mod21Δ alp16Δ* multiple mutant relative to single or double mutants, in both *mod22+* and *mod22-1* backgrounds, is that each of the nonessential γ-TuC proteins might be required for the others to be stable in vivo or for them to associate with a small γ-TuC containing γ-tubulin, alp4p, and alp6p. For example, in *Xenopus* γ-TuRC reconstitution experiments, immunodepletion of GCP6 from salt-dissociated γ-TuRC has been shown to prevent the reassembly of large complexes (Zhang *et al.*, 2000). We therefore examined association dependencies of gfh1p, mod21p, and alp16p with the γ-TuC, by performing coimmunoprecipitation experiments in a variety of mutant backgrounds (Figure 10).

We found that mod21-Myc could be coimmunoprecipitated with alp4-HA only when both gfh1p and alp16 were present, and this was also true for coimmunoprecipitation of mod21-Myc with alp6-HA (Figure 10A). By contrast, coimmunoprecipitation of gfh1-Myc with either alp4-HA or alp6-HA required the presence of alp16p, but not mod21p (Figure 10B). The *mod22-1* mutation did not affect the coimmunoprecipitation of either gfh1-Myc or mod21-Myc with alp4-HA or alp6-HA. These experiments also showed that cytoplasmic levels of all of the proteins of interest are not significantly altered in the mutants under study and that interactions of γ-tubulin with alp4p and alp6p remain intact in these mutants.

Table 3. Astral microtubules are not released from spindle poles in *gfh1*Δ, *mod21*Δ, and additional mutants

Strain	Relevant genotype	GFP-atb2p	Total cells observed	Total astral microtubule histories	Histories with length = 1 frame	Histories with length >1 frame	Histories with length >1 frame and astral MT release
KS1236	Wild type	Alone	6	18	11	7	0
KS1225	Wild type	With *atb2+*	7	27	5	22	0 (1?)[a]
KS1704	*gfh1*Δ	Alone	4	13	4	9	0
KS1708	*gfh1*Δ	With *atb2+*	4	22	9	13	0
KS1720	*gfh1*Δ *mod22-1*	Alone	9	25	6	19	0
KS1727	*gfh1*Δ *mod22-1*	With *atb2+*	7	12	1	11	1 (2?)
KS1696	*mod21*Δ	Alone	9	18	5	13	0 (1?)
KS1701	*mod21*Δ	With *atb2+*	11	46	5	41	1
KS1724	*mod21*Δ *mod22-1*	Alone	7	33	9	24	0
KS1733	*mod21*Δ *mod22-1*	With *atb2+*	10	42	9	33	1 (2?)
KS1812	*alp16*Δ *gfh1*Δ *mod21*Δ *mod22-1*	Alone	10	44	13	31	0
KS1817	*alp16*Δ *gfh1*Δ *mod21*Δ *mod22-1*	With *atb2+*	22	98	16	82	2–4[b]

Thirty-second frame intervals were used throughout for data acquisition and measurement. Further details can be found in *Materials and Methods*. Cells were scored from the time of spindle formation up to the beginning of formation of the PAA from the eMTOC.

[a] (?) includes astral microtubules (MTs) that may have released, but only when eMTOC was already considerably active in forming the PAA, and thus cell cycle-dependent changes in microtubule behavior may already be occurring at the SPB.

[b] In two of these instances, spindles had elongated all the way to cell tips and astral MTs were forced to bend; in the other two instances, two successive release events were observed in one individual cell, both from the same spindle pole.

In further experiments, we found that the coimmunoprecipitation of alp16-Myc with alp4-HA was dependent on gfh1p but not on mod21p (Figure 11A), and also that levels of alp16p were not altered in *gfh1*Δ or *mod21*Δ strains. Subject to the caveats associated with using tagged strains (see *Materials and Methods* and Supplemental Tables 1–3), we conclude from these results that association dependencies can account for at least some of the similar phenotypes seen among single and multiple deletions of *gfh1+*, *mod21+* and *alp16+*, although, notably, both gfh1p and alp16p still associate with the small γ-TuC proteins in *mod21*Δ mutants.

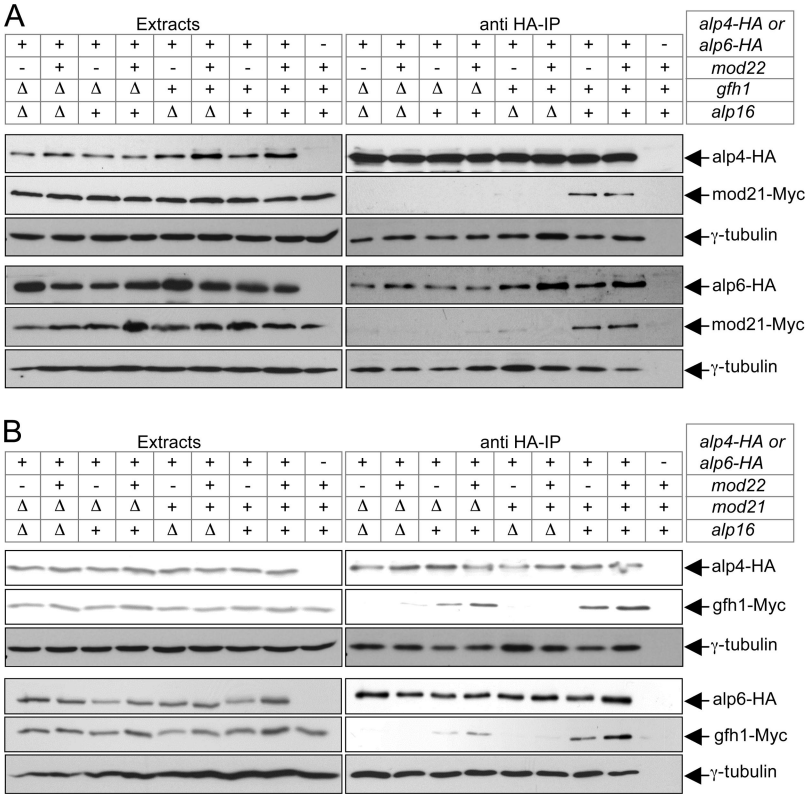

Figure 10. Association of mod21p with γ-TuC requires both gfh1p and alp16p, whereas association of gfh1p with γ-TuC requires only alp16p. Anti-HA coimmunoprecipitations of Myc-tagged mod21p (A) or Myc-tagged gfh1p with HA-tagged γ-TuC components alp4p or alp6p (B), in strains with the indicated genotypes. *alp4-HA* and *alp6-HA* strains were used in separate experiments, with the results from *alp4-HA* strains shown in the top panels of A and B, and the results from *alp6-HA* strains shown in the bottom panels of A and B. For *alp4-HA* and *alp6-HA*, "−" indicates negative control strains with untagged protein; for *mod22*, "−" indicates the *mod22-1* allele. For other genes, wild-type or deletion alleles are as indicated.

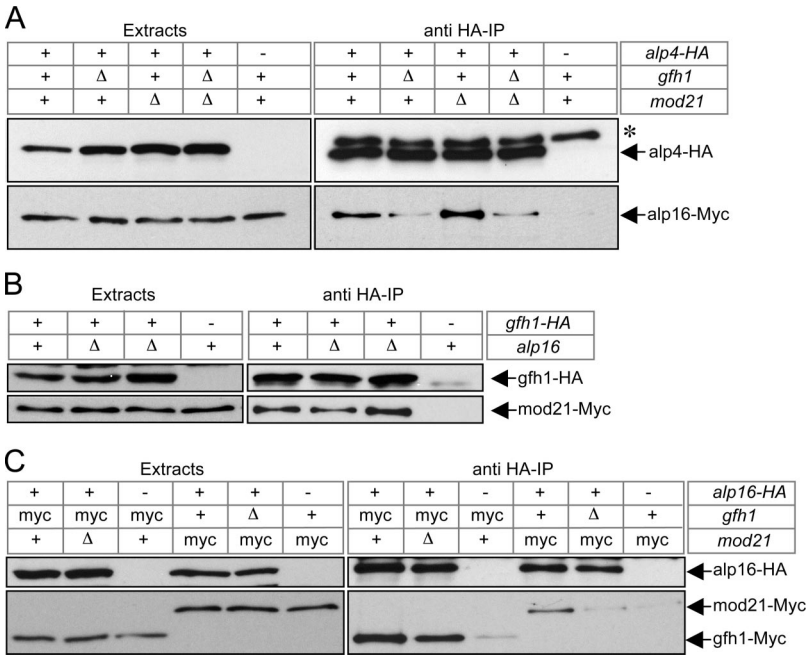

Figure 11. gfh1p and mod21p can associate independent of alp16p or the γ-TuC. (A) Anti-HA coimmunoprecipitation of Myc-tagged alp16p with HA-tagged alp4p in strains with the indicated genotypes. alp16-Myc is only weakly associated with alp4-HA in *gfh1*Δ strains. Asterisk marks a nonspecific band that is occasionally but not always enriched in immunoprecipitates, depending on time of exposure of Western blots (compare with Figures 2 and 10). (B) Anti-HA coimmunoprecipitation of Myc-tagged mod21p with HA-tagged gfh1p in *alp16+* and *alp16*Δ mutants. Mod21p and gfh1p coimmunoprecipitate in *alp16*Δ, i.e., even when they are not associated with the γ-TuC (see Figure 10). The two identical central lanes represent two different strain isolates of *gfh1-HA mod21-Myc alp16*Δ. (C) Anti-HA coimmunoprecipitation of Myc-tagged gfh1p or Myc-tagged mod21p with HA-tagged alp16p in strains of the indicated genotypes. Mod21p does not associate with alp16p in *gfh1*Δ strains (i.e., when mod21p and alp16p are not associated with γ-TuC), whereas gfh1p does associate with alp16p in *mod21*Δ strains (i.e., when both gfh1p and alp16p are associated with γ-TuC).

Interestingly, gfh1-HA and mod21-Myc coimmunoprecipitated in *alp16*Δ mutants (Figure 11B), even though neither gfh1p nor mod21p would be expected to associate with the small γ-TuC proteins under these conditions (Figure 10). By contrast, alp16p was not associated with mod21p in the absence of gfh1p (Figure 11C). In the same experiment, we found that alp16p did associate with gfh1p in the absence of mod21p, but we note that under these conditions, both gfh1p and alp16p are themselves associated with the small γ-TuC (Figures 10B and 11, A and C). Together, these results suggest that assembly of a larger γ-TuC in fission yeast may involve the interdependent association of distinct subcomplexes, including a gfh1p–mod21p subcomplex, although we note in this context that the gfh1-HA allele is likely to have impaired function (see *Materials and Methods* and Supplemental Tables 1–3).

As described above, our analysis of mutant phenotypes indicates that many γ-TuC–dependent microtubule behaviors are essentially intact in fission yeast when multiple subunits and/or regulators of the γ-TuC are absent (*gfh1*Δ,

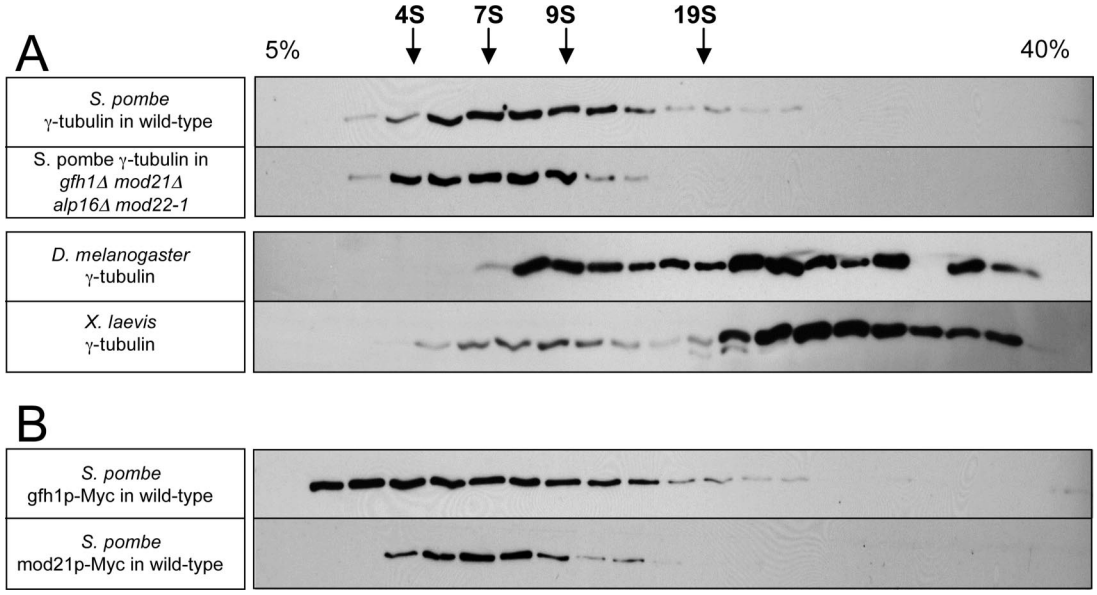

Figure 12. Fission yeast γ-tubulin is mostly present in a small complex on sucrose gradients. Western blots of cell extracts after sucrose gradient sedimentation. (A) Untagged γ-tubulin in extracts from wild-type and *gfh1*Δ *mod21*Δ *alp16*Δ *mod22-1* fission yeast as well as from *Drosophila* embryos and *Xenopus* eggs. (B) Myc-tagged gfh1p, and, independently, Myc-tagged mod21p, in extracts from wild-type fission yeast. The top of the gradient is at the left, and the positions of S-value standards are indicated above the top panel. The gap in staining near the bottom of the *Drosophila* extract gradient is due to a loading error.

*mod21*Δ, and *alp16*Δ) or mutated (*mod22-1*). This led us to wonder whether these subunits might not always be tightly associated with the γ-TuC in vivo; that is, whether a significant fraction of functional γ-TuCs in wild-type cells might in fact be small complexes. Previous analysis of the fission yeast γ-TuC by gel filtration chromatography has produced ambiguous and/or conflicting results concerning the size of wild-type and mutant complexes (Vardy and Toda, 2000; Fujita *et al*., 2002; Venkatram *et al*., 2004; see *Discussion*). We therefore followed a complementary approach to analyze the γ-TuC, by using sucrose gradient sedimentation.

Using the buffer conditions of our coimmunoprecipitation experiments, we found that nearly all γ-tubulin in wild-type fission yeast extracts was present in a relatively low S-value complex, ~8–9S, and this was not significantly altered in a *gfh1*Δ *mod21*Δ *alp16*Δ *mod22-1* strain (Figure 12A). As controls, we prepared *Drosophila* embryo extracts and *Xenopus* egg extracts, using the same buffers as for fission yeast (see *Materials and Methods*). As reported previously, *Drosophila* γ-tubulin sedimented in both small and large complexes, whereas *Xenopus* γ-tubulin sedimented mostly as a large complex (Stearns and Kirschner, 1994; Oegema *et al*., 1999). Both gfh1p and mod21p also sedimented with low S-values, albeit reproducibly differently from each other (Figure 12B and Supplemental Figure 6). From these data, it could not be confirmed that either gfh1p or mod21p was comigrating with γ-tubulin. Overall, our results suggest that, in contrast to γ-tubulin from higher eukaryotes, most of the γ-tubulin in fission yeast cell extracts is not detected in large protein complexes, even when the homologues of GCP4 (gfh1p), GCP5 (mod21p), and GCP6 (alp16p) are present. This could reflect a lower abundance of large complexes in vivo or a reduced stability of large complexes in vitro.

On extended exposure of Western blots of sucrose gradients, a very small amount of fission yeast γ-tubulin seemed to sediment in a larger complex, >20S, that occurred as a "bump" on the shoulder of the broad small S-value peak (Supplemental Figure 5, asterisk). Small amounts of gfh1p and mod21p were also reproducibly enriched at this position, and the γ-tubulin bump was no longer apparent in the *gfh1*Δ *mod21*Δ *alp16*Δ *mod22-1* mutant (Supplemental Figure 5). Although these results might suggest that the bump represents an intact large fission yeast γ-TuC, this should be viewed with caution, because sedimentation profiles of alp4p or alp6p did not routinely show such a distinct bump (Supplemental Figure 5). Another reason for caution in interpreting such high S-value forms of γ-tubulin is that in further experiments involving higher resolution gradients and longer centrifugation times, we observed not only the small 8–9S form of γ-tubulin seen previously but also a prominent higher S-value form that seemed to be distinct from the higher S-value form observed with shorter centrifugation times (Supplemental Figure 6, asterisks). Curiously, no other γ-TuC components comigrated with this new larger form, which was equally present in both wild-type cells and *gfh1*Δ *mod21*Δ *alp16*Δ *mod22-1* mutants (Supplemental Figure 6). This suggests that fission yeast γ-tubulin may be subject to aggregation artifacts under certain conditions in vitro.

DISCUSSION

Understanding how the various components of the multisubunit γ-TuC contribute to its function is a major outstanding question in microtubule nucleation. Our characterization of mod21p, together with gfh1p and alp16p (Fujita *et al*., 2002; Venkatram *et al*., 2004), supports the notion that fission yeast can form a large γ-TuC similar to that found in higher eukaryotes and that this complex is important for maintaining normal levels of microtubule nucleation in vivo. At the same time, however, two findings in particular lead us to propose that the nonessential proteins gfh1p, mod21p, and alp16p should be considered as noncore components of the γ-TuC, in contrast to the essential core components γ-tubulin, alp4p and alp6p. First, we have found that most qualitative aspects of microtubule nucleation persist in vivo when all noncore components of the γ-TuC are deleted, the major observed difference being a quantitative reduction in interphase microtubule nucleation activity. This stands in marked contrast to the very strong nucleation-defective phenotypes observed upon loss of nonessential proteins that recruit the γ-TuC to prospective cytoplasmic nucleation sites, such as mto1p or mto2p (Sawin *et al*., 2004; Venkatram *et al*., 2004, 2005; Janson *et al*., 2005; Samejima *et al*., 2005). Second, we have not found evidence for an abundant high S-value γ-TuC containing the noncore components, even in wild-type cells; rather, we observe nearly all γ-tubulin in low S-value forms (see below for further discussion).

Roles of Novel Components mod21+ and mod22+

Because both gfh1p and alp16p are required for association of mod21p with the γ-TuC, it is difficult to judge whether the three noncore subunits have distinct functions. However, we note that the association of both gfh1p and alp16p with the γ-TuC is independent of mod21p, whereas the association of mod21p with the γ-TuC depends on both gfh1p and alp16p, and the loss of mod21p phenocopies simultaneous loss of all three noncore subunits. In this light, mod21p may merit special attention as the most "peripheral" and the least "architectural" of the noncore subunits. Further mutational analysis of noncore components will help to address these issues.

In this work, we also identified genetically an additional regulator of γ-TuC function, *mod22+*. The identification of *mod22-1* was not only fortuitous but also essential to our identification of *mod21+* in a morphological mutant screen. Because the *mod22-1* phenotype is strongest when noncore components are deleted, it seems plausible that *mod22+* may function to promote the nucleation efficiency of a small core γ-TuC. Although *mod22+* has not yet been cloned, our results to date indicate that *mod22* is not allelic to any known components of the γ-TuC or to any of the three tubulin genes in fission yeast (our unpublished data).

Function of gfh1p, mod21p, and alp16p in Microtubule Nucleation and Organization

Our analysis of the noncore subunits suggests that they can be treated together as a single functional class in relation to regulating microtubule behavior. In the area of microtubule nucleation, we have shown that loss of one, two, or all three noncore subunits does not disrupt microtubule nucleation from any of the three different types of MTOCs normally present in vivo. This in turn indicates that an intact large γ-TuC is broadly dispensable for microtubule nucleation in fission yeast (Fujita *et al*., 2002; Venkatram *et al*., 2004). It is possible that the reduced iMTOC nucleation observed in deletion mutants is due to the loss of a specific but as yet unrecognized subclass of iMTOCs; further higher-resolution work will be required to address this.

Altered microtubule dynamics have been observed in many fission yeast mutants affecting microtubule nucleation, particularly γ-TuC mutants (Paluh *et al*., 2000; Vardy and Toda, 2000; Fujita *et al*., 2002; Sawin *et al*., 2004; Venkatram *et al*., 2004, 2005; Janson *et al*., 2005; Zimmerman and Chang, 2005). In all of our mutants, microtubules within

bundles were seen to turn over, but the bundles themselves had longer lifetimes than in wild-type cells, accompanied by oscillations of SPBs. The mechanistic reasons for these differences in bundle behavior and/or structure are not yet clear. Such differences could be an indirect consequence of reduced microtubule nucleation (Sawin *et al*., 2004; Samejima *et al*., 2005), driven, for example, by a higher ratio of bundling proteins relative to bundles. Alternatively, if microtubule minus-ends were normally capped by γ-TuCs in wild-type fission yeast, but not in our mutants, minus-ends might be more free to elongate and become bundled. Although we observed the γ-TuC marker alp4-GFP associated with microtubules in our mutants, we do not know whether its localization may be subtly altered.

In our experiments, we did not quantitate parameters of dynamic instability of individual microtubules, partly because important dynamic instability transitions may occur deep within bundles rather than at the ends of bundles (making them very difficult to observe) and also because the bundles in mutant cells may themselves have a different polarity and/or organization relative to wild-type cells. It is still unclear whether the alterations in dynamics that have been observed in microtubule-nucleation mutants arise primarily as an indirect consequence of nucleation defects or whether nucleation complexes themselves play a more direct role in modulating microtubule dynamics (Paluh *et al*., 2000; Sawin *et al*., 2004; Zimmerman and Chang, 2005). Further work is needed to resolve this important issue.

In contrast to the previous results of Venkatram *et al*. (2004), we did not observe significant release of astral microtubules from SPBs during mitosis in any of our mutants. The reason for this discrepancy is not clear. Very early PAA microtubules that translocate from their nucleation sites could be mistaken for released astral microtubules, but we observed such microtubules equally frequently in wild-type and mutant cells. The results of Venkatram *et al*. (2004)could be due to aberrantly high levels of GFP-tubulin expression. In their work, GFP-atb2p was expressed from a multi-copy plasmid, using the very high-strength *nmt1* promoter under fully derepressed conditions (Venkatram, personal communication), whereas we used two integrated versions of GFP-atb2p, expressed at near to or slightly lower than physiological levels. In previous work, we demonstrated that some mutant strains defective in microtubule nucleation can be supersensitive to GFP-tubulin levels (Sawin *et al*., 2004).

The Fission Yeast γ-TuC in Relation to Higher Eukaryotes

In spite of extensive biochemical studies of the γ-TuC in several different organisms, there are still questions as to which form(s) of the complex may be active for nucleation in vivo, and in what contexts. In budding yeast, where homologues of GCP4, GCP5 and GCP6 have not been identified, the active form of γ-TuC is thought to be the ~11S Tub4 complex, anchored to the SPB (Knop *et al*., 1997; Vinh *et al*., 2002). In metazoan cells, both small and large γ-TuCs can be identified in cell extracts to varying extents, the ~30–35S γ-TuRC being a much more potent nucleator in vitro than the smaller ~10S γ-TuSC subcomplex, perhaps by 2 orders of magnitude (Oegema *et al*., 1999). Because the γ-TuRC has been seen to form a cap on nucleated microtubules (Moritz *et al*., 2000) and is by far the predominant form of γ-tubulin in vertebrate cells, a general view has emerged that the γ-TuRC is the primary microtubule nucleator in higher eukaryotes, for both centrosomal and noncentrosomal nucleation. However, while our paper was under review, Verrolet *et al*. (2006) published a study on the role of the *Drosophila* homologues of GCP4, GCP5, and GCP6 in microtubule nucleation in vivo (Verollet *et al*., 2006). In this work, γ-tubulin targeting and microtubule nucleation at the centrosome were still preserved after combined RNA interference knockdowns of these three γ-TuRC–specific proteins, suggesting that the γ-TuSC is sufficient for at least some aspects of microtubule nucleation in higher eukaryotes. However, it is unclear whether γ-TuSC–mediated nucleation would normally function alongside γ-TuRC–mediated nucleation in untreated cells (Verollet *et al*., 2006).

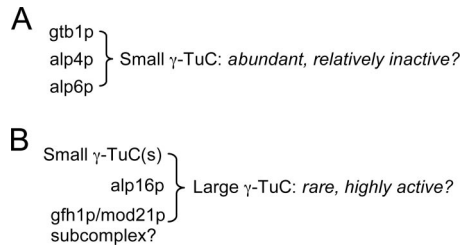

Figure 13. γ-TuC organization and function in fission yeast. Schematic view that attempts to reconcile the phenotypic consequences of deletion of noncore γ-TuC components gfh1p, mod21p, and/or alp16p (i.e., reduced interphase microtubule nucleation) with our inability to detect a significant pool of large γ-TuCs on sucrose gradients. In this view, the fission yeast γ-TuC may exist as two populations: a small, abundant, but weakly active complex lacking noncore components (A); and a larger, much less abundant, but much more active complex containing noncore components, including a subcomplex of gfh1p and mod21p (B). In wild-type cells, both types of complexes could contribute to total microtubule nucleation.

What is the situation in fission yeast? Our sucrose gradient data suggest that a large proportion of the γ-TuC in wild-type fission yeast may be in the form of small complexes, with perhaps only a very small fraction in larger, canonical complexes containing noncore subunits. How can we reconcile this with our phenotype analysis showing that cells without noncore subunits nucleate microtubules reasonably well from all types of MTOCs but are nevertheless partially defective in interphase nucleation? One interesting, albeit speculative, possibility is that there may be a "division of labor" between large and small γ-TuCs in fission yeast (Figure 13). According to this view, wild-type cells may contain a relatively small number of large γ-TuCs, which contain noncore subunits and are highly active for microtubule nucleation, and a much greater number of small γ-TuCs, which lack noncore subunits and are less active for nucleation. In this manner, the two pools of γ-TuCs could each contribute a significant amount of the total interphase microtubule nucleation activity. In relation to other systems, this view would put fission yeast somewhere "in between" higher eukaryotes, which rely primarily or exclusively on the γ-TuRC (possibly because of the need to nucleate hundreds of microtubules), and budding yeast, which have only the equivalent of the small γ-TuSC. Because budding yeast nucleate cytoplasmic microtubules only from the SPB, it is also noteworthy that loss of noncore components in fission yeast does not restrict cytoplasmic nucleation to the SPB, because this indicates that the differences between budding and fission yeast with regard to nucleation are not simply explained by the presence/absence of noncore components. Further work will be necessary to test these ideas in detail.

It is also important to acknowledge that the physical nature of the fission yeast γ-TuC in vivo is not yet certain. In particular, Fujita *et al*. (2002) found that the fission yeast γ-TuC behaved as a very large complex by gel filtration, and its size was unaffected by *alp16*Δ (Fujita *et al*., 2002). This is

paradoxical, partly because our immunoprecipitation experiments indicate that loss of alp16p from the complex should lead to loss of gfh1p and mod21p as well. In addition, Venkatram *et al*. (2004) have shown that under the buffer conditions of Fujita *et al*. (2002), both wild-type and mutant γ-TuCs exceed the exclusion limit of the column used by both groups (Superose 6). In these experiments, the use of low ionic strength buffers containing both glycerol and ATP could have led to unintentional aggregation of a small γ-TuC. Indeed, in our own experiments, we found conditions that seemed to aggregate γ-tubulin artificially, and changes in buffer conditions have also been noted to alter the size of the budding yeast Tub4 complex on sucrose gradients (Vinh *et al*., 2002). It is also possible that in our experiments a large complex was unintentionally disrupted. However, our coimmunoprecipitation and sucrose gradient experiments used the same buffers, and these also preserved the state of the higher-eukaryotic γ-TuRC. Thus, at minimum, it is likely that an association of γ-TuC noncore components with core-components is less robust in fission yeast than in higher eukaryotes. It remains to be seen whether such a weaker association would be constitutive or perhaps regulated by labile posttranslational modifications (e.g., phosphorylation), which might not survive cell extraction.

ACKNOWLEDGMENTS

We thank T. Toda and O. Niwa for providing yeast strains, S. MacNeill and A. Carr for tagging cassettes, and K. Gull and I. Stancheva for antibodies. We also thank H. Ohkura, I. Samejima, H. Snaith, and S. Venkatram for useful discussions and/or comments on the manuscript. K.E.S. is a Wellcome Trust Senior Research Fellow in Basic Biomedical Sciences. This work was supported by the Wellcome Trust.

REFERENCES

Bahler, J., Wu, J. Q., Longtine, M. S., Shah, N. G., McKenzie, A., 3rd, Steever, A. B., Wach, A., Philippsen, P., and Pringle, J. R. (1998). Heterologous modules for efficient and versatile PCR-based gene targeting in *Schizosaccharomyces pombe*. Yeast *14*, 943–951.

Basi, G., Schmid, E., and Maundrell, K. (1993). TATA box mutations in the *Schizosaccharomyces pombe*nmt1 promoter affect transcription efficiency but not the transcription start point or thiamine repressibility. Gene *123*, 131–136.

Chen, C. R., Li, Y. C., Chen, J., Hou, M. C., Papadaki, P., and Chang, E. C. (1999). Moe1, a conserved protein in *Schizosaccharomyces pombe*, interacts with aRas effector, Scd1, to affect proper spindle formation. Proc. Natl. Acad. Sci. USA *96*, 517–522.

Chikashige, Y., Kurokawa, R., Haraguchi, T., and Hiraoka, Y. (2004). Meiosis induced by inactivation of Pat1 kinase proceeds with aberrant nuclear positioning of centromeres in the fission yeast *Schizosaccharomyces pombe*. Genes Cells *9*, 671–684.

Cormack, B. P., Valdivia, R. H., and Falkow, S. (1996). FACS-optimized mutants of the green fluorescent protein (GFP). Gene *173*, 33–38.

Ding, D. Q., Chikashige, Y., Haraguchi, T., and Hiraoka, Y. (1998). Oscillatory nuclear movement in fission yeast meiotic prophase is driven by astral microtubules, as revealed by continuous observation of chromosomes and microtubules in living cells. J. Cell Sci. *111*, 701–712.

Drummond, D. R., and Cross, R. A. (2000). Dynamics of interphase microtubules in *Schizosaccharomyces pombe*. Curr. Biol. *10*, 766–775.

Fava, F., Raynaud-Messina, B., Leung-Tack, J., Mazzolini, L., Li, M., Guillemot, J. C., Cachot, D., Tollon, Y., Ferrara, P., and Wright, M. (1999). Human 76p: a new member of the gamma-tubulin-associated protein family. J. Cell Biol. *147*, 857–868.

Fujita, A., Vardy, L., Garcia, M. A., and Toda, T. (2002). A fourth component of the fission yeast gamma-tubulin complex, Alp16, is required for cytoplasmic microtubule integrity and becomes indispensable when gamma-tubulin function is compromised. Mol. Biol. Cell *13*, 2360–2373.

Goldstein, A. L., and McCusker, J. H. (1999). Three new dominant drug resistance cassettes for gene disruption in *Saccharomyces cerevisiae*. Yeast *15*, 1541–1553.

Gunawardane, R. N., Lizarraga, S. B., Wiese, C., Wilde, A., and Zheng, Y. (2000). gamma-tubulin complexes and their role in microtubule nucleation. Curr. Top. Dev. Biol. *49*, 55–73.

Hagan, I. M. (1998). The fission yeast microtubule cytoskeleton. J. Cell Sci. *111*, 1603–1612.

Hentges, P., Van Driessche, B., Tafforeau, L., Vandenhaute, J., and Carr, A. M. (2005). Three novel antibiotic marker cassettes for gene disruption and marker switching in *Schizosaccharomyces pombe*. Yeast *22*, 1013–1019.

Horio, T., Uzawa, S., Jung, M. K., Oakley, B. R., Tanaka, K., and Yanagida, M. (1991). The fission yeast gamma-tubulin is essential for mitosis and is localized at microtubule organizing centers. J. Cell Sci. *99*, 693–700.

Janson, M. E., Setty, T. G., Paoletti, A., and Tran, P. T. (2005). Efficient formation of bipolar microtubule bundles requires microtubule-bound gamma-tubulin complexes. J. Cell Biol. *169*, 297–308.

Job, D., Valiron, O., and Oakley, B. (2003). Microtubule nucleation. Curr. Opin. Cell Biol. *15*, 111–117.

Keating, T. J., and Borisy, G. G. (1999). Centrosomal and non-centrosomal microtubules. Biol Cell *91*, 321–329.

Knop, M., Pereira, G., Geissler, S., Grein, K., and Schiebel, E. (1997). The spindle pole body component Spc97p interacts with the gamma-tubulin of *Saccharomyces cerevisiae* and functions in microtubule organization and spindle pole body duplication. EMBO J. *16*, 1550–1564.

Knop, M., and Schiebel, E. (1998). Receptors determine the cellular localization of a gamma-tubulin complex and thereby the site of microtubule formation. EMBO J. *17*, 3952–3967.

Masuda, H., Miyamoto, R., Haraguchi, T., and Hiraoka, Y. (2006). The carboxy-terminus of Alp4 alters microtubule dynamics to induce oscillatory nuclear movement led by the spindle pole body in *Schizosaccharomyces pombe*. Genes Cells *11*, 337–352.

Mata, J., and Nurse, P. (1997). tea1 and the microtubular cytoskeleton are important for generating global spatial order within the fission yeast cell. Cell *89*, 939–949.

Moreno, S., Klar, A., and Nurse, P. (1991). Molecular analysis of the fission yeast *Schizosaccharomyces pombe*. Methods Enzymol. *194*, 795–823.

Moritz, M., Braunfeld, M. B., Guenebaut, V., Heuser, J., and Agard, D. A. (2000). Structure of the gamma-tubulin ring complex: a template for microtubule nucleation. Nat. Cell Biol. *2*, 365–370.

Murphy, S. M., Preble, A. M., Patel, U. K., O'Connell, K. L., Dias, D. P., Moritz, M., Agard, D., Stults, J. T., and Stearns, T. (2001). GCP5 and GCP6, two new members of the human gamma-tubulin complex. Mol. Biol. Cell *12*, 3340–3352.

Murphy, S. M., Urbani, L., and Stearns, T. (1998). The mammalian gamma-tubulin complex contains homologues of the yeast spindle pole body components spc97p and spc98p. J. Cell Biol. *141*, 663–674.

Oakley, B. R. (2000). gamma-Tubulin. Curr. Top. Dev. Biol. *49*, 27–54.

Oegema, K., Wiese, C., Martin, O. C., Milligan, R. A., Iwamatsu, A., Mitchison, T. J., and Zheng, Y. (1999). Characterization of two related *Drosophila* gamma-tubulin complexes that differ in their ability to nucleate microtubules. J. Cell Biol. *144*, 721–733.

Paluh, J. L., Nogales, E., Oakley, B. R., McDonald, K., Pidoux, A. L., and Cande, W. Z. (2000). A. mutation in gamma-tubulin alters microtubule dynamics and organization and is synthetically lethal with the kinesin-like protein pkl1p. Mol. Biol. Cell *11*, 1225–1239.

Pardo, M., and Nurse, P. (2005). The nuclear rim protein Amo1 is required for proper microtubule cytoskeleton organisation in fission yeast. J. Cell Sci. *118*, 1705–1714.

Samejima, I., Lourenco, P. C., Snaith, H. A., and Sawin, K. E. (2005). Fission yeast mto2p regulates microtubule nucleation by the centrosomin-related protein mto1p. Mol. Biol. Cell *16*, 3040–3051.

Sawin, K. E., Lourenco, P. C., and Snaith, H. A. (2004). Microtubule nucleation at non-spindle pole body microtubule-organizing centers requires fission yeast centrosomin-related protein mod20p. Curr. Biol. *14*, 763–775.

Sawin, K. E., and Mitchison, T. J. (1991). Mitotic spindle assembly by two different pathways in vitro. J. Cell Biol. *112*, 925–940.

Sawin, K. E., and Nurse, P. (1996). Identification of fission yeast nuclear markers using random polypeptide fusions with green fluorescent protein. Proc. Natl. Acad. Sci. USA *93*, 15146–15151.

Sawin, K. E., and Nurse, P. (1998). Regulation of cell polarity by microtubules in fission yeast. J. Cell Biol. *142*, 457–471.

Sawin, K. E., and Snaith, H. A. (2004). Role of microtubules and tea1p in establishment and maintenance of fission yeast cell polarity. J. Cell Sci. *117*, 689–700.

Sawin, K. E., and Tran, P. T. (2006). Cytoplasmic microtubule organization in fission yeast. Yeast *23*, 1001–1014.

Schiebel, E. (2000). gamma-Tubulin complexes: binding to the centrosome, regulation and microtubule nucleation. Curr. Opin. Cell Biol. *12*, 113–118.

Snaith, H. A., and Sawin, K. E. (2003). Fission yeast mod5p regulates polarized growth through anchoring of tea1p at cell tips. Nature *423*, 647–651.

Stearns, T., Evans, L., and Kirschner, M. (1991). Gamma-Tubulin is a highly conserved component of the centrosome. Cell *65*, 825–836.

Stearns, T., and Kirschner, M. (1994). In vitro reconstitution of centrosome assembly and function: the central role of gamma-tubulin. Cell *76*, 623–637.

Tanaka, K., Kohda, T., Yamashita, A., Nonaka, N., and Yamamoto, M. (2005). Hrs1p/Mcp6p on the meiotic SPB organizes astral microtubule arrays for oscillatory nuclear movement. Curr. Biol. *15*, 1479–1486.

Tran, P. T., Marsh, L., Doye, V., Inoue, S., and Chang, F. (2001). A. mechanism for nuclear positioning in fission yeast based on microtubule pushing. J. Cell Biol. *153*, 397–411.

Vardy, L., and Toda, T. (2000). The fission yeast gamma-tubulin complex is required in G(1) phase and is a component of the spindle assembly checkpoint. EMBO J. *19*, 6098–6111.

Venkatram, S., Jennings, J. L., Link, A., and Gould, K. L. (2005). Mto2p, a novel fission yeast protein required for cytoplasmic microtubule organization and anchoring of the cytokinetic actin ring. Mol. Biol. Cell *16*, 3052–3063.

Venkatram, S., Tasto, J. J., Feoktistova, A., Jennings, J. L., Link, A. J., and Gould, K. L. (2004). Identification and characterization of two novel proteins affecting fission yeast gamma-tubulin complex function. Mol. Biol. Cell *15*, 2287–2301.

Verollet, C., Colombie, N., Daubon, T., Bourbon, H. M., Wright, M., and Raynaud-Messina, B. (2006). *Drosophila melanogaster* gamma-TuRC is dispensable for targeting gamma-tubulin to the centrosome and microtubule nucleation. J. Cell Biol. *172*, 517–528.

Vinh, D. B., Kern, J. W., Hancock, W. O., Howard, J., and Davis, T. N. (2002). Reconstitution and characterization of budding yeast gamma-tubulin complex. Mol. Biol. Cell *13*, 1144–1157.

Wilde, A., and Zheng, Y. (1999). Stimulation of microtubule aster formation and spindle assembly by the small GTPase Ran. Science *284*, 1359–1362.

Zhang, L., Keating, T. J., Wilde, A., Borisy, G. G., and Zheng, Y. (2000). The role of Xgrip210 in gamma-tubulin ring complex assembly and centrosome recruitment. J. Cell Biol. *151*, 1525–1536.

Zheng, Y., Wong, M. L., Alberts, B., and Mitchison, T. (1995). Nucleation of microtubule assembly by a gamma-tubulin-containing ring complex. Nature *378*, 578–583.

Zimmerman, S., and Chang, F. (2005). Effects of {gamma}-tubulin complex proteins on microtubule nucleation and catastrophe in fission yeast. Mol. Biol. Cell *16*, 2719–2733.

Zimmerman, S., Tran, P. T., Daga, R. R., Niwa, O., and Chang, F. (2004). Rsp1p, a J domain protein required for disassembly and assembly of microtubule organizing centers during the fission yeast cell cycle. Dev. Cell *6*, 497–509.